[20]L. Yuan, Paper at Intern. Symposium on Transition Radiation of High Energy Particles, Erevan (1977).
[21]Trudy Mezhdunarodnogo simpoziuma po perekhodnomu izlucheniyu chastits vysokoĭ énergii, Erevan, 1977 (Proc. Intern. Symposium on Transition Radiation of High Energy Particles, Erevan, 1977), Erevan Physics Institute (1977).
[22]E. L. Feinberg, Usp. Fiz. Nauk **58**, 193 (1956).
[23]M. I. Ryazanov, Zh. Eksp. Teor. Fiz. **65**, 123 (1973) [Sov. Phys. JETP **38**, 61 (1974)].
[24]H. A. Bethe and E. E. Salpeter, Quantum Mechanics of One and Two Electron Atoms, Springer, Berlin (1957) [Russian translation published by Fizmatgiz, Moscow (1960)].
[25]V. M. Galitskiĭ and I. I. Gurevich, Nuovo Cimento **32**, 396 (1964).
[26]L. D. Landau and I. Ya. Pomeranchuk, Dokl. Akad. Nauk SSSR **92**, 535, 735 (1953).
[27]A. B. Migdal, Zh. Eksp. Teor. Fiz. **32**, 633 (1957) [Sov. Phys. JETP **5**, 527 (1957)].
[28]M. I. Ryazanov, Usp. Fiz. Nauk **114**, 393 (1974) [Sov. Phys. Usp. **17**, 815 (1975)].
[29]N. Bohr, The Penetration of Atomic Particles Through Matter, Hafner (1948) [Russian translation published in Moscow (1965)].
[30]J. Neufeld and R. H. Ritchie, Phys. Rev. **98**, 1632 (1965).
[31]V. H. Neelavathi and R. H. Ritchie, in: Atomic Collisions in Solids, Vol. 50, Plenum, New York (1975), p. 289.
[32]Z. Vager and D. S. Gemmel, Phys. Rev. Lett. **37**, 1352 (1976).
[33]Z. Vager, D. S. Gemmel, and B. J. Zabransky, Phys. Rev. A **14**, 638 (1976).
[34]W. Brandt, A. Ratkovski, and R. H. Ritchie, Phys. Rev. Lett. **33**, 1325 (1974).
[35]W. Brandt and R. H. Ritchie, Nucl. Instrum. Methods **132**, 43 (1976).
[36]W. Brandt, R. Laubert, and A. Ratkowski, Nucl. Instrum. Methods **132**, 57 (1976).
[37]J. M. Tape *et al.*, Nucl. Instrum. Methods **132**, 75 (1976).
[38]D. S. Gemmel *et al.*, Nucl. Instrum. Methods **132**, 61 (1976).
[39]Yu. Kagan, Yu. V. Kononets, and N. K. Dzhamankyzov, Zh. Eksp. Teor. Fiz. **74**, 288 (1978) [Sov. Phys. JETP **47**, 148 (1978)].
[40]V. L. Ginzburg and V. N. Tsytovich, Phys. Rep. **49**, 1 (1979) [Russian translation published in Usp. Fiz. Nauk **126**, 553 (1978)].
[41]D. Pines, Elementary Excitations in Solids, Benjamin, New York (1963) [Russian translation published by Mir, Moscow (1965)].
[42]V. P. Silin and A. A. Rukhadze, Élektromagnitnye svoĭstva plazmy i plazmopodobnykh sred (Electromagnetic Properties of Plasmas and Plasma-like Media, Atomizdat, Moscow (1961).
[43]N. R. Arista and V. H. Ponce, J. Phys. C **8**, 188 (1975).
[44]N. R. Arista, Phys. Rev. B **18**, 1 (1978).
[45]R. Laubert and F. K. Chen, Bull. Am. Phys. Soc. **24** (1), 25 (1979).
[46]M. I. Ryazanov, Zh. Eksp. Teor. Fiz. **43**, 1559 (1962) [Sov. Phys. JETP **16**, 1100 (1963)].
[47]M. I. Ryazanov, Zh. Eksp. Teor. Fiz. **48**, 1490 (1965) [Sov. Phys. JETP **21**, 997 (1965)].
[48]K. A. Barsukov and B. M. Bolotovskiĭ, Zh. Eksp. Teor. Fiz. **45**, 303 (1964) [Sov. Phys. JETP **18**, 211 (1964)].
[49]S. A. Akhmanov and R. V. Khokhlov, Problemy nelineĭnoĭ optiki (Problems of Nonlinear Optics), Moscow.
[50]N. Bloembergen, Nonlinear Optics, Benjamin, New York (1965) [Russian translation published by Mir, Moscow (1966)].
[51]P. D. McWane and D. A. Sealer, Appl. Phys. Lett. **8**, 278 (1966).
[52]P. D. Maker and P. W. Terhune, Phys. Rev. **137**, A801 (1965).
[53]M. I. Ryazanov, Pis'ma Zh. Eksp. Teor. Fiz. **15**, 437 (1972) [JETP Lett. **15**, 310 (1972)].
[54]Yu. S. Kalashnikova, Zh. Eksp. Teor. Fiz. **71**, 2085 (1976) [Sov. Phys. JETP **44**, 1096 (1976)].
[55]V. K. Lyapidevskiĭ and M. I. Ryazanov, Pis'ma Zh. Eksp. Teor. Fiz. **32**, 516 (1980) [JETP Lett. **32**, 496 (1980)].
[56]V. S. Butylkin *et al.*, Rezonansnye vzaimodeĭstviya sveta s veshchestvom (Resonance Interactions of Light with Matter), Nauka, Moscow (1977).
[57]S. P. Andreev and M. I. Ryazanov, Dokl. Akad. Nauk SSSR **215**, 807 (1974) [Sov. Phys. Dokl. **19**, 191 (1974)].
[58]D. B. Rogozkin and M. I. Ryazanov, Zh. Eksp. Teor. Fiz. **80**, No. 6 (1981).

Translated by Julian B. Barbour

Multiparticle production in hadron–nucleus collisions at high energies

Yu. M. Shabel'skiĭ

B. P. Konstantinov Institute of Nuclear Physics, Leningrad
Fiz. Elem. Chastits At. Yadra **12**, 1070–1115 (September–October 1981)

Multiparticle production processes on nuclei at high energies are discussed in the framework of the model of multiple scattering and the composite quark model. The various forms of these models and their connections are analyzed. It is shown that they permit an explanation of the experimentally observed phenomena and make a number of quantitative predictions in good agreement with the experiments. Consideration is given to the possibility of extracting from the experimental data information about the properties of strong interactions, in particular, about the formation time of the secondary particles. The structure of the quark–quark amplitude is analyzed. Arguments are put forward supporting the view that the spatial distribution of the matter in hadrons is inhomogeneous, and the possibilities of further study of the phenomenon are discussed.

PACS numbers: 13.85.Hd, 12.40.Bb, 11.80.La

INTRODUCTION

The ever increasing interest in multiparticle production of hadrons on nuclei is due in the first place to the possibility of obtaining unique information about the properties of the strong interactions. There have long been indications[1-3] that the production of particles on nuclei does not occur as in an ordinary extended target, for which the interaction probabilities of the primary particle and the secondary particles are determined solely by their cross sections and the matter density. Interest in hadron–nucleus collisions quickened abruptly with the appearance of the parton model,[4-5] according to which the interaction of a hadron moving with momentum p requires the time

$$\tau \sim p/\mu^2, \qquad (1)$$

where μ is the characteristic scale of the strong interactions. Then, as was noted by Kancheli,[6] the secondary particles of sufficiently high energy produced in the nucleus will not be rescattered by the nuclear nucleons, since for this there is not sufficient time. As we shall see, the available experimental data agree with such behavior and place a restriction on the value of μ. Subsequently, in Refs. 7–13, it was shown that the quark structure of hadrons is clearly manifested in multiparticle production on nuclei.

In the present review, the main attention is devoted to the problem of extracting from the experimental data information about the spatial distribution of the quarks and gluons within hadrons, about the structure of the quark–quark amplitude, and the formation time of the secondary particles. In Sec. 1, we discuss the theoretical ideas which provide the basis of the various models of hadron–nucleus collisions. In Sec. 2, we consider the basic experimental facts—the behavior of the inelastic cross sections, the mean multiplicities, and the inclusive spectra of the secondary particles. More detailed experimental data are given later as they need to be compared with the results of calculations. Section 3 is devoted to formulating the model of multiple scattering and comparing its predictions with the experiments. In Sec. 4, we discuss the manifestation of the composite quark structure of hadrons when they interact with nuclei. The model of multiple scattering and the quark model are compared in Sec. 5, in which various possible mechanisms of the quark–nucleus interaction are considered. In Sec. 6, we discuss cascade rescattering of spectator quarks of the target and the influence of such processes on the contribution of double interactions to hadron–deuteron collisions. In Sec. 7, we discuss deep inelastic scattering of leptons on nuclei and formation time of secondary particles.

1. BASIC THEORETICAL IDEAS ABOUT THE MECHANISM OF HADRON–NUCLEUS INTERACTIONS

To extract information about the properties of the strong interactions from experimental data on hadron–nucleus collisions, it is necessary to determine the main mechanism of particle production on nuclei at high energies. There currently exist many models which treat hadron–nucleus collisions from the most varied points of view. First of all, we must mention the intranuclear cascade model,[14,15] in which it is assumed that the secondary particles arise within the nucleus instantaneously and then are immediately capable of interacting. All the calculations are made in the classical limit, i.e., probabilities rather than amplitudes are added. At initial energies not exceeding a few GeV, the cascade model was used to describe a large number of experimental data (though here too further and more detailed testing of the model is very desirable). At higher energies, the cascade has too many branches and strongly overestimates[15] the multiplicities of the secondary particles.

One of the ways of eliminating the contradiction with the experiments is to introduce the finite formation time (1) of the secondary particles; during this time, they virtually do not interact, and only comparatively slow secondary particles participate in the cascade multiplication process. This results in a parton–hadron cascade.[16] The multiplicity of secondary particles of moderate energy is appreciably higher in the case of a nucleus than on a nucleon on account of the contribution of the cascades, while the multiplicities of fast particles on a nucleus and on a nucleon must be

 0090-4759/81/050430-19$02.80

equal. The value of the parameter μ^2 in (1) can be found experimentally and is ~2 GeV^2.[16]

In both models, it was assumed that the entire difference between the multiparticle production processes on a nucleus and on a nucleon arises from the cascade rescattering of the secondary particles. However, this probably does not correspond to reality. For example, we regard a hadron as a system of two or three spatially separated quarks and assume that in a collision with a nucleon a single quark interacts as a rule, i.e., the impulse approximation is satisfied.[17,18] In the case of collisions with nuclei, the probabilities for the interaction of two or three quarks are not small,[7-12] so that the multiplicity of the secondary particles in the case of a nucleus will be greater than for a nucleon whatever the formation time of the secondary particles.

The quark structure of hadrons was taken into account in the framework of a hadron–parton cascade model in Refs. 19 and 20, in which it was assumed that the multiplicity of secondary particles in the case of nuclei is increased, first, by the greater mean number of interacting quarks and, second, by the cascade rescattering of the secondary particles of moderate energy. To achieve agreement with experiment, it was necessary[19,20] to reduce the cascade contribution to a value characterized by $\mu^2 = 0.5$–0.7 GeV^2 (secondary particles produced with momentum $\gtrsim 30$ GeV/c effectively undergo no rescattering in any existing nucleus). The calculations in Refs. 19 and 20 were made under the assumption that the multiplicity and all the other characteristics are the same in quark–nucleon and quark–nucleus interactions.

This last hypothesis may also be incorrect. If the quark–nucleon interaction is determined by the sum of several different mechanisms, their relative contributions may depend on A (as, for example, in the considered case of the quark model, in which the probability of interactions of one quark decreases with increasing A but the probability of interaction of two or three increases). In the theory of complex angular momenta the interaction is constructed in this way, and besides Reggeon exchange corresponding to the production of one multiperipheral ladder there is a cut contribution corresponding to the formation of several such ladders.[21,22] The latter contribution increases with increasing A, with the consequence that the multiplicity of the secondary particles in a quark-nucleus interaction must be higher than in the case of a nucleon. These ideas provide the basis of the multiple-scattering model, various aspects of which are considered in Refs. 23–30. In this model, the mean multiplicity, the multiplicity distributions, the inclusive spectra, the two-particle correlations, and a number of other characteristics of hadron–nucleus collisions can be described without any contribution of intranuclear cascades, which corresponds to a very small value of the parameter μ in (1).

In the multiple-scattering model, it is necessary to make an assumption about the structure of the multi-Reggeon vertices (in other words, about the distribution of energy between the different Reggeons). Asymptotically, all variants must give the same results (excluding the fragmentation region of the incident particle), but at the accessible energies the differences may be appreciable. In particular, one variant of the model takes into account the composite quark structure of hadrons. Another variant has become known as the leading-particle cascade model and is considered in Refs. 31–34.

Finally, in a large group of models the hadron-nucleus interaction is not reduced to a superposition of hadron–nucleon interactions. In some of the models,[35-38] the incident particle interacts at once with all the nucleons in a tube of cross section $\sim\sigma_{\text{inel}}^{hN}$; in others,[39-41] it is assumed that in the first collision clusters are formed which interact with the nucleons of the nucleus and are only then transformed into secondary particles. As a rule, these models describe the experiments reasonably well, but there is considerable arbitrariness in their formulation. Because of limitations of space, such models will not be considered in this review.

2. GENERAL EXPERIMENTAL FACTS ON HADRON–NUCLEUS INTERACTIONS

A. Cross sections of inelastic processes. All possible processes involving the collision of high-energy hadrons with nuclei can be nominally divided into five groups:

$$\sigma_{\text{el}}^{hA} = \sigma(h + A \to h + A); \tag{2}$$

$$\sigma_{\text{diss}}^{hA} = \sigma(h + A \to h + A^*); \tag{3}$$

$$\sigma_{\text{coh}}^{hA} = \sigma(h + A \to h^* + A); \tag{4}$$

$$\sigma_{\text{noncoh}}^{hA} = \sigma(h + A \to h^* + A^*); \tag{5}$$

$$\sigma_{\text{abs}}^{hA} = \sigma(h + A \to \text{hadrons}). \tag{6}$$

The process (2) is ordinary elastic scattering, (3) is incoherent elastic scattering accompanied by excitation or dissociation of the nucleus, (4) is the coherent production of a resonance or beam of particles, (5) is incoherent diffraction production on individual nucleons, and (6) is ordinary multiparticle production.

We also define the cross section of all processes without production of secondary particles [(2) and (3)],

$$\sigma_{\text{scat}}^{hA} = \sigma_{\text{el}}^{hA} + \sigma_{\text{diss}}^{hA}, \tag{7}$$

and the total cross section of the processes (4)–(6) with

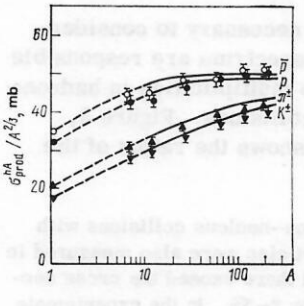

FIG. 1. Cross sections for production of secondary particles on nuclei for different beams at 200 GeV/c. The curves are calculated in accordance with Eq. (10).

the production of at least one secondary particle:

$$\sigma_{\text{prod}}^{hA} = \sigma_{\text{abs}}^{hA} + \sigma_{\text{coh}}^{hA} + \sigma_{\text{noncoh}}^{hA} = \sigma_{\text{tot}}^{hA} - \sigma_{\text{scat}}^{hA}. \quad (8)$$

It is this cross section which will be our main concern.

The values of $\sigma_{\text{prod}}^{hA}$ for $\pi^{\pm}$, $K^{\pm}$, $\bar{p}$, and p beams at 60, 200, and 280 GeV were measured in Ref. 42 for different targets. Their energy dependence in this range is very weak. The values of $\sigma_{\text{prod}}^{hA}$ at 200 GeV are given in Fig. 1. It can be seen that for $A \geq 30$ the values of $\sigma_{\text{prod}}^{pA}$ and $\sigma_{\text{prod}}^{\bar{p}A}$ are proportional to $A^{2/3}$, whereas for meson beams they increase much more rapidly.[1)]

The cross sections $\sigma_{\text{prod}}^{hA}$ can be calculated with good accuracy in the optical model. Suppose a fast hadron collides with a nucleus with impact parameter b. The probability of its passage through the nucleus without inelastic interaction with the nuclear nucleons, i.e., without the production of secondary particles, is given by the expression $\exp[-\sigma_{\text{inel}}^{hN} T(b)]$, where

$$T(b) = A \int_{-\infty}^{\infty} \rho(b, z)\, dz, \quad (9)$$

in which $\rho(r = \sqrt{b^2 + z^2})$ is the density distribution of the nuclear matter. Then we obtain the cross section (8) in the form

$$\sigma_{\text{prod}}^{hA} = \int d^2b \{1 - \exp[-\sigma_{\text{inel}}^{hN} T(b)]\}. \quad (10)$$

Figure 1 shows the calculated values of $\sigma_{\text{prod}}^{hA}$ (10) obtain- using the cross sections $\sigma_{\text{inel}}^{hN}$ taken from Ref. 44 and the Fermi distribution of the nuclear density:

$$\left.\begin{aligned} &\rho(r) = \rho_0 \left[1 + \exp\left(\frac{r - c_1}{c_2}\right)\right]^{-1}; \quad \int \rho(r)\, 4\pi r^2\, dr = 1, \\ &c_1 = 1.15 \text{ F } A^{1/3}, \quad c_2 = 0.51 \text{ F}. \end{aligned}\right\} \quad (11)$$

It can be seen that the results of the calculation agree reasonably with experiment.

B. Mean multiplicities of charged particles. The overwhelming majority of the secondary hadrons produced on nuclei (excluding some of the protons and pions in the target fragmentation region) are so-called s particles. The A dependence of the multiplicities $\langle n_s \rangle_{pA}$ and $\langle n_s \rangle_{\pi^- A}$ (based on the data collected together in Ref. 30) at initial energy 200 GeV is shown in Fig. 2. For $A \gtrsim 10$, the multiplicities can be parametrized by the power-law dependence $\langle n_s \rangle \sim A^{\alpha}$ with $\alpha \sim 0.2$ for a π^--meson beam and a somewhat larger value for a proton beam. As was pointed out in Ref. 38, such a value of α is an argument against the collective tube model,[35-37] for which one expects $\alpha \sim 1/10$–$1/12$.

C. Inclusive spectra. It is necessary to consider what regions of the inclusive spectrum are responsible for the difference between the multiplicities in hadron–nucleus and hadron–nucleon collisions. Figure 3, which is taken from Ref. 47, shows the ratios of the

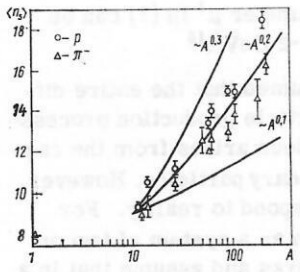

FIG. 2. Mean multiplicities of relativistic charged particles in pA and $\pi^- A$ collisions at 200 GeV.

inclusive spectra on an average photoemulsion nucleus and on a nucleon as functions of the variable $\eta = -\ln\tan\theta_{\text{lab}}/2$, which is close to the value $y = \frac{1}{2}\ln\frac{E + p_{\parallel}}{E - p_{\parallel}}$ used in theoretical studies. As can be seen from Fig. 3, in the central region and even more in the target fragmentation region the multiplicities of particles produced on a nucleus are much higher than those on a nucleon. However, in the beam fragmentation region their ratio, $R(hA/hN)$, is appreciably less than unity, and, to within the errors, the size of this region does not depend on the initial energy. As we shall show below, this behavior is characteristic for the multiple-scattering model and for the quark model and contradicts the predictions of the parton model,[16] and also models based on Reggeon diagrams of "tree" type (see, for example, Ref. 48).

The A dependence of the inclusive spectra in the beam fragmentation region is shown in more detail in Fig. 4, in which we have plotted the ratios of the multiplicities of secondary $\pi^{\pm}$, $K^{\pm}$, $\bar{p}$, and p at 24 GeV/c, 17 mrad,[49] and Λ and K_s^0 at 300 GeV/c, 0.25 mrad,[50] in p Pb and p Be collisions. It can be seen that the ratios are virtually independent of the species of the secondary particles (excluding, perhaps, K^+ mesons) and the initial energy and become less than unity at $x \gtrsim 1/5$.

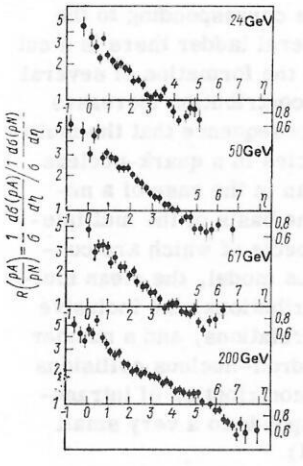

FIG. 3. Ratios of the spectra of charged particles on photoemulsion nuclei and on the nucleon as functions of the quasirapidity η for different energies of the incident proton.

[1)] The cross sections (8) of neutron–nucleus collisions with the production of secondary particles were also measured in Ref. 43, but the values obtained there exceed the cross sections $\sigma_{\text{prod}}^{pA}$ and $\sigma_{\text{inel}}^{pp}$ (Ref. 44) by 2–5%. In the experiments with the Serpukhov accelerator,[45,46] the cross section including the processes (3) with disintegration of the nucleus was evidently measured.

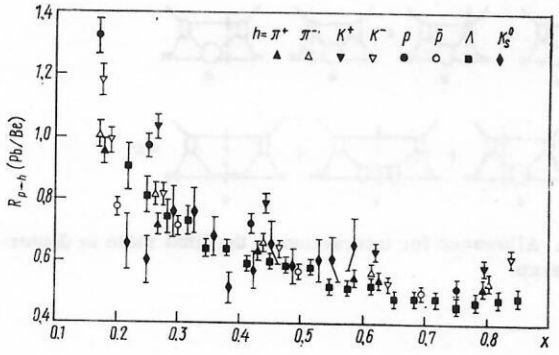

FIG. 4. Ratios of the multiplicities of different hadrons in pPb and pBe collisions as functions of x.

3. MULTIPARTICLE PRODUCTION ON NUCLEI IN THE MULTIPLE-SCATTERING MODEL

A. Elastic scattering of hadrons on nuclei. At moderate energy (~1 GeV), elastic scattering of hadrons by nuclei can be described with good accuracy by the Glauber model.[51] If for simplicity we ignore the difference between the amplitudes of hadron scattering by the proton and by the neutron, $f_p(q)=f_n(q)=f(q)$, and also the real part of $f(q)$ and the center-of-mass motion of the nucleus, the amplitude of elastic hadron–nucleus scattering has in accordance with Ref. 51 the form

$$F_{\mathrm{Gl}}(q)=\frac{ik}{2\pi}\int \Gamma_{\mathrm{Gl}}(b)\exp(iqb)\,d^2b; \tag{12}$$

$$\Gamma_{\mathrm{Gl}}(b)=1-\sum_{n=0}^{A} C_A^n\left[\frac{i}{2\pi k}\int \exp(-iqb)\,f(q)\,G(q)\,d^2q\right]^n, \tag{13}$$

where

$$C_A^n=\frac{A!}{n!\,(A-n)!}; \quad G(q)=\int \exp(iqs)\,d^2s\int \rho(s,\,z)\,dz \tag{14}$$

is the single-particle nuclear form factor, $\rho(r)$ is the distribution of the nuclear density, and k is the momentum of the initial hadron. It is assumed that the incident particle is scattered successively by the nucleons of the nucleus and that the total phase shift is the sum of the phase shifts from the individual nucleons.

If the initial energy is increased, the space-time structure of the interaction changes. In accordance with the ideas of the parton model[4-6] the interaction time becomes greater than the time taken by the fast particle to pass through the nucleus, and then successive interactions with several nucleons are impossible and all interactions take place at the same time. Scattering of high-energy hadrons by nuclei was investigated by Gribov,[52] who showed that in this case it is necessary to take into account not only the elastic shadowing corrections but also the inelastic shadowing. The presence of the latter does not mean that a real resonance or a diffraction beam of particles moves through the nucleus. In reality, these states, like the pole contributions corresponding to elastic shadowing, are intermediate states in the unitarity condition for the amplitude of elastic scattering of a Reggeon by a hadron,[53] and this, in accordance with Ref. 52, determines the magnitude of the shadowing corrections. One can here draw a parallel with the ordinary elastic scattering of hadrons, which does not at all proceed through the production and subsequent absorption of real secondary particles despite the fact that the unitarity condition contains contributions of mulitparticle intermediate states.

At the attainable energies of 10^2–10^3 GeV, the contribution of inelastic shadowing is not numerically large, but it is desirable to take it into account. The point is that from energies ~10 GeV onward coherent diffraction production of beams of particles on nuclei occurs. The inelastic shadowing in the case of heavy nuclei essentially reduces to allowance for such processes in the intermediate states, and therefore the neglect of such shadowing would be inconsistent. One of the simple ways of taking into account the inelastic shadowing corrections is by means of the two-channel model,[54,55] according to which the amplitude $f(q)$ in (13) must be replaced by the matrix

$$Bf(q)=\begin{vmatrix}1 & g\\ g & \delta\end{vmatrix} f(q), \tag{15}$$

where the parameter g is determined by the ratio of the cross sections for production on a nucleon of a diffraction beam, $h+N\to X+N$, and for elastic scattering, and also by the nuclear form factor, which takes into account the longitudinal momentum transfer q_z. At moderate energies, q_z becomes large and $g\to 0$. The parameter δ describes a beam–beam transition, and in the following numerical calculations it is taken equal to unity.

The direct use of Eqs. (12)–(15) leads to lengthy calculations for the cross sections of the processes in which we are interested. For a Gaussian distribution of the nuclear matter, they are given in Ref. 23. However, the expressions simplify considerably in the "optical" limit, when the range of the strong interactions is ignored compared with the radius of the nucleus and allowance is made for $A\gg 1$. Actually, such neglect is possible already with $A\sim 10$. We take $f(q)$ in front of the integral in (13) at the value $q=0$ [$f(0)=ik\sigma/(4\pi)$, where σ is the total cross section of the hadron–nucleon interaction]. Substituting (14) and (15) and setting $C_A^n\approx A^n/n!$, we obtain the amplitudes of elastic scattering and coherent production in the form

$$\left.\begin{aligned}F_{\mathrm{el}}(\sigma,\,q)&=\tfrac{1}{2}(1+\cos\theta)\,F_{\mathrm{Gl}}(\lambda_1\sigma,\,q)\\&+\tfrac{1}{2}(1-\cos\theta)\,F_{\mathrm{Gl}}(\lambda_2\sigma,\,q);\\F_{\mathrm{coh}}(\sigma,\,q)&=\tfrac{1}{2}\sin\theta\,[F_{\mathrm{Gl}}(\lambda_1\sigma,\,q)-F_{\mathrm{Gl}}(\lambda_2\sigma,\,q)],\end{aligned}\right\} \tag{16}$$

where

$$F_{\mathrm{Gl}}(\sigma,\,q)=\frac{ik}{2\pi}\int\left\{1-\exp\left[-\frac{\sigma}{2}T(b)\right]\right\}\exp(iqb)\,d^2b$$

is the ordinary Glauber amplitude of elastic scattering, and

$$\lambda_{1,2}=\tfrac{1}{2}(1+\delta\pm X);\ X^2=(1-\delta)^2+4g^2;\ \cos\theta=(1-\delta)/X.$$

The integrated cross sections of elastic scattering and coherent production on the nucleus take the form

$$\sigma_{\mathrm{el}}^{hA}=\int d^2b\left\{1-\frac{1+\cos\theta}{2}\exp\left[-\tfrac{1}{2}\lambda_1\sigma T(b)\right]-\frac{1-\cos\theta}{2}\exp\left[-\tfrac{1}{2}\lambda_2\sigma T(b)\right]\right\}^2; \tag{17}$$

$$\sigma_{\mathrm{coh}}^{hA}=\frac{\sin^2\theta}{4}\int d^2b\left\{\exp\left[-\tfrac{1}{2}\lambda_1\sigma T(b)\right]-\exp\left[-\tfrac{1}{2}\lambda_2\sigma T(b)\right]\right\}^2, \tag{18}$$

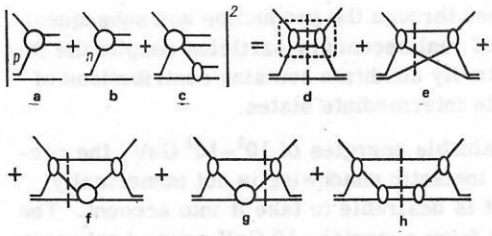

FIG. 5. Deuteron breakup cross section in the impulse approximation.

and the total cross section is

$$\sigma_{\text{tot}}^{hA}=2\int d^2b\left\{1-\frac{1+\cos\theta}{2}\exp\left[-\frac{1}{2}\lambda_1\sigma T(b)\right]-\frac{1-\cos\theta}{2}\exp\left[-\frac{1}{2}\lambda_2\sigma T(b)\right]\right\}. \tag{19}$$

At moderate energies, there is no inelastic shadowing, which corresponds to the limit $g\to 0$, and $\lambda_1=1,\lambda_2=\delta$, $\cos\theta=1$.

B. Diagram method of determining the cross sections of incoherent processes. If the elastic-scattering amplitude is known, the cross sections of incoherent processes can in principle be found by means of the unitarity condition, which relates the imaginary part of the elastic amplitude to the sum of the cross sections of all the channels. As an example, we calculate the cross section for deuteron breakup by a fast hadron, $h+d\to h+p+n$, with allowance for interaction of the nucleons in the final state, i.e., we find the square of the modulus of the sum of the amplitudes corresponding to Figs. 5a–5c (the contribution of the more complicated graphs can be found similarly).

It can be seen directly[2)] that the sum of the squares of the moduli of the amplitudies for Figs. 5a and 5b is equal to the contribution of the impulse approximation to the total cross section, $2\sigma_{\text{tot}}^{hN}$, multiplied by the ratio $\sigma_{\text{el}}^{hN}/\sigma_{\text{tot}}^{hN}$, since not all the intermediate but only the elastic states are taken in the hN scattering block within the dotted line in Fig. 5d. The interference of the amplitudes corresponding to Figs. 5a and 5b is equal to the contribution of the shadowing correction (Fig. 5e) to the total cross section, and we ignore it. The total contribution of the square of the modulus of the amplitude for Fig. 5c and its interference with the amplitudes for Figs. 5a and 5b (this contribution is shown in Figs. 5f–5h) can be determined as follows. Consider the imaginary part of the amplitude in Fig. 6a. It is equal to the sum of the six different absorptive parts shown in Figs. 6b–6g. At the same time, the contribution of the graph in Fig. 6a to the total hd cross section is negligibly small[56] (since, as a rule, the nucleons do not have time to interact while the fast particle is passing through the deuteron). The absorptive parts shown in Figs. 6b and 6c contain to the right or left of the division amplitudes which are small for

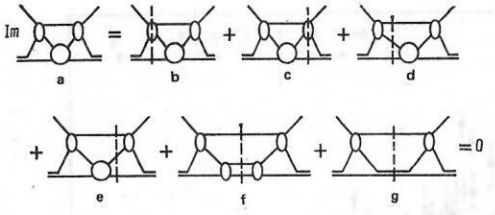

FIG. 6. Allowance for interaction in the final state in deuteron breakup.

the same reason. Therefore, the sum of the remaining absorptive parts is also zero, i.e., the required sum of three of them (Figs. 6d–6f) is equal to the absorptive part (Fig. 6g) taken with the opposite sign. And the latter is equal to the contribution of the impulse approximation to the cross section $\sigma_{\text{el}(1)}^{hd}$ of elastic hd scattering.

Thus, allowance for the interaction of the nucleons in the final state decreases the deuteron dissociation cross section $\sigma_{\text{diss}}^{hd}$ by the amount $\sigma_{\text{el}(1)}^{hd}$:

$$\sigma_{\text{diss}}^{hd}=\sigma_{\text{el}}^{hp}+\sigma_{\text{el}}^{hn}-\sigma_{\text{el}}^{hd},$$

which, apart from the shadowing corrections, agrees with the direct calculation in the Glauber model.[57]

Note that the total cross section of elastic scattering and disintegration, σ_{scat} (7), is not changed by allowance for nucleon rescattering. It can be shown (see, for example, Refs. 23 and 58) that in the case of multiparticle production the interaction in the final state also does not change the integrated cross sections but merely changes the angular and energy distributions of the secondary particles.

C. Cross sections of incoherent processes. Using the completeness condition for the nuclear wave functions, it is possible to calculate[23] the total cross section of coherent and incoherent diffraction excitation of the incident hadron, i.e., the sum of (4) and (5). For $A\gg 1$, it has the form

$$\sigma_{\text{diff}}^{hA}=\sigma_{\text{coh}}^{hA}+\sigma_{\text{noncoh}}^{hA}=\frac{\sin^2\theta}{4}\int d^2b\left\{\exp\left[-\lambda_1\sigma_1^{in}T(b)\right]+\exp\left[-\lambda_2\sigma_2^{in}T(b)\right]-2\exp\left[-(\lambda_1+\lambda_2)\sigma_hT(b)\right]\right\}, \tag{20}$$

where

$$\sigma_{1,2}^{in}=\sigma-\lambda_{1,2}\sigma_{\text{el}};\quad \sigma_h=\sigma-2\frac{\lambda_1\lambda_2}{\lambda_1+\lambda_2}\sigma_{\text{el}};\quad \sigma_{\text{el}}=\sigma_{\text{el}}^{hN}.$$

The total cross section of all the binary processes (2)–(5) can be calculated[23] similarly and is

$$\sigma_{\text{bin}}^{hA}=\sigma_{\text{tot}}^{hA}-\sigma_{\text{abs}}^{hA}=\frac{1+\cos\theta}{2}\int d^2b\left\{1-2\exp\left[-\frac{1}{2}\lambda_1\sigma T(b)\right]+\exp\left[-\lambda_1\sigma_1^{in}T(b)\right]\right\}+\frac{1-\cos,\theta}{2}\int d^2b\left\{1-2\exp\left[-\frac{1}{2}\lambda_2\sigma T(b)\right]+\exp\left[-\lambda_2\sigma_2^{in}T(b)\right]\right\}. \tag{21}$$

It is convenient to classify the various processes in hadron–nucleus collisions on the basis of the number of cut hadron–nucleon blocks in the elastic hadron–nucleus amplitude (in other words, on the basis of the number of nucleons of the nucleus to which a momentum $q\gg 1/R_A$ is transferred). For example, the cross

[2)] The broken curve in Fig. 5 and below denotes a "division" or "cutting" of the graph: The amplitude of the process shown on the left of the cut line is multiplied by the complex-conjugate amplitude of the process shown on the right and integrated over the internal momenta.

section (21) can be represented as the sum of the contributions $\sigma_{\text{bin}}^{(l)}$, where l is the number of cut blocks, the contribution of all the cuts between the blocks ($l=0$) being

$$\sigma_{\text{bin}}^{(0)}=\frac{1+\cos\theta}{2}\int d^2b\left\{1-\exp\left[-\frac{1}{2}\lambda_1\sigma T(b)\right]\right\}^2+\frac{1-\cos\theta}{2}\int d^2b\left\{1-\exp\left[-\frac{1}{2}\lambda_2\sigma T(b)\right]\right\}^2. \quad (22)$$

This contribution is equal to the sum of σ_{el}^{hA} (17) and σ_{coh}^{hA} (18), and for $l>0$

$$\sigma_{\text{bin}}^{(l)}=\frac{1+\cos\theta}{2}\int d^2b\,\frac{1}{l!}\left[\sigma_{\text{el}}\lambda_1^2T(b)\right]^l\exp\left[-\lambda_1\sigma T(b)\right]+\frac{1-\cos\theta}{2}\int d^2b\,\frac{1}{l!}\left[\sigma_{\text{el}}\lambda_2^2T(b)\right]^l\exp\left[-\lambda_2\sigma T(b)\right]. \quad (23)$$

From this, we can go over to the cross sections of the multiple processes. The cross section corresponding to production of particles on ν nucleons of the nucleus and elastic scattering on $l-\nu$ nucleons has the form[23]

$$\sigma_{\text{abs}}^{(l,\nu)}=\frac{1}{l!}C_l^\nu\left\{\frac{1+\cos\theta}{2}\left(\frac{\sigma_1^{in}}{\lambda_1\sigma_{\text{el}}}\right)^\nu\int d^2b\left[\lambda_1^2\sigma_{\text{el}}T(b)\right]^l\exp\left[-\lambda_1\sigma T(b)\right]+\frac{1-\cos\theta}{2}\left(\frac{\sigma_2^{in}}{\lambda_2\sigma_{\text{el}}}\right)^\nu\int d^2b\left[\lambda_2^2\sigma_{\text{el}}T(b)\right]^l\exp\left[-\lambda_2\sigma T(b)\right]\right\}. \quad (24)$$

Summing over l, we obtain the cross section for inelastic interaction with ν nucleons in the form

$$\sigma_{\text{abs}}^{(\nu)}=\frac{1+\cos\theta}{2}\int d^2b\,\frac{1}{\nu!}\left[\lambda_1\sigma_1^{in}T(b)\right]^\nu\exp\left[-\lambda_1\sigma_1^{in}T(b)\right]+\frac{1-\cos\theta}{2}\int d^2b\,\frac{1}{\nu!}\left[\lambda_2\sigma_2^{in}T(b)\right]^\nu\exp\left[-\lambda_2\sigma_2^{in}T(b)\right]. \quad (25)$$

Finally, the total cross section of the multiparticle processes (6) is

$$\sigma_{\text{abs}}^{hA}=\sum_{\nu=1}^{\infty}\sigma_{\text{abs}}^{(\nu)}=\int d^2b\left\{1-\frac{1+\cos\theta}{2}\exp\left[-\lambda_1\sigma_1^{in}T(b)\right]-\frac{1-\cos\theta}{2}\exp\left[-\lambda_2\sigma_2^{in}T(b)\right]\right\}. \quad (26)$$

In the absence of inelastic shadowing, the cross sections of inelastic interaction with ν nucleons (25) take the well-known form

$$\sigma_{\text{prod}}^{(\nu)}=\sigma_{\text{abs}}^{(\nu)}=\frac{1}{\nu!}\int d^2b\left[\sigma_{\text{in}}T(b)\right]^\nu\exp\left[-\sigma_{\text{in}}T(b)\right],\quad \sigma_{\text{in}}=\sigma_{\text{inel}}^{hN}. \quad (27)$$

They can be represented in the form[23]

$$\sigma_{\text{prod}}^{(\nu)}=\sum_{n=\nu}^{\infty}\Delta_nB_n^{(\nu)},\quad B_n^{(\nu)}=(-1)^{n+\nu}2^{n-1}C_n^\nu\left(\frac{\sigma_{\text{in}}}{\sigma}\right)^n, \quad (28)$$

where

$$\Delta_n=2\int d^2b\,\frac{1}{n!}\left[\frac{\sigma T(b)}{2}\right]^n \quad (29)$$

is the contribution of n-fold interaction to σ_{tot}^{hA} (19):

$$\sigma_{\text{tot}}^{hA}=\sum_{n=1}^{\infty}(-1)^{n+1}\Delta_n.$$

The $B_n^{(\nu)}$ values determine the contribution of graphs containing n hadron–nucleon blocks, with ν of them cut, to the cross sections $\sigma_{\text{prod}}^{(\nu)}$, i.e., they determine the relations between the different absorptive parts of the different graphs. The analogous expressions for Reggeon graphs were found in Ref. 59. The obtained values $B_n^{(\nu)}$ (28) differ from the corresponding coefficients in Ref. 59 only by the factor $(\sigma_{\text{in}}/\sigma)^n$, which arises from the possibility of both two-particle and many-particle cuts of the hadron–nucleon blocks.

In the absence of inelastic shadowing, the expression (24) can also be written in the form

$$\sigma_{\text{prod}}^{(l,\nu)}=\sum_{n=l}^{\infty}B_n^{(l,\nu)}\Delta_n,\quad B_n^{(l,\nu)}=(-1)^{n+1}2^{n-1}C_n^lC_l^\nu\times\left(\frac{\sigma_{\text{in}}}{\sigma}\right)^\nu\left(\frac{\sigma_{\text{el}}}{\sigma}\right)^{l-\nu}. \quad (30)$$

The representations (28) and (30) will also be true for light nuclei (including the deuteron) if we calculate the Δ_n, the contributions to σ_{tot}^{hA}, using the exact expressions and not the approximation (29), which holds when $A\gg1$. However, in (28) and (30) the ratio of the range of the strong interactions to the radius of the nucleus is ignored.

When allowance is made for inelastic shadowing in the two-channel model, $B_n^{(\nu)}$ and $B_n^{(l,\nu)}$ become much more complicated. However, one can assume with good accuracy that only the contributions Δ_n change, while the values of $B_n^{(\nu)}$ and $B_n^{(l,\nu)}$ do not.

D. Inclusive spectra. We consider first the central region of the spectrum. If we ignore the violations of scaling in the hadron–nucleon spectra, then on the cutting of the ν blocks there can be the necessary secondary particle in each of them, and therefore the contribution to the ratio of the multiplicities on the nucleus and on the nucleon will be equal to $\nu\sigma_{\text{abs}}^{(\nu)}/\sigma_{\text{abs}}^{hA}$. Summing with allowance for (25), we obtain

$$R\left(\frac{hA}{hN}\right)=\frac{n_{hA}(y)}{n_{hN}(y)}=\sum_{\nu=1}^{\infty}\frac{\nu\sigma_{\text{abs}}^{(\nu)}}{\sigma_{\text{abs}}^{hA}}=\langle\nu\rangle_{hA}=A\frac{\sigma_m}{\sigma_{\text{abs}}^{hA}}, \quad (31)$$

where $\sigma_m=\sigma-(1+g^2)\sigma_{\text{el}}$ is the total inelastic hN cross section, with the cross section of diffraction dissociation of the incident hadron subtracted. In the absence of inelastic shadowing, (31) goes over into the widely used expression

$$R\left(\frac{hA}{hN}\right)=\langle\nu\rangle_{hA}=A\frac{\sigma_{\text{inel}}^{hN}}{\sigma_{\text{prod}}^{hA}}. \quad (32)$$

For real nuclei, the numerical difference between (31) and (32) does not exceed 2–3%.

In the projectile fragmentation region, the ratio $R(hA/hN)$ must decrease by virtue of energy conservation.[23,24,60] For example, in one event there cannot be more than one particle with $x>\frac{1}{2}$ more than two with $x>\frac{1}{3}$ and so forth. Suppose a fast baryon interacts, exchanging Pomerons, with two nuclear nucleons. The contributions to the elastic-scattering amplitude for this case are shown in Figs. 7a and 7b, the former being the simplest Mandelstam graph, while the latter is more complicated. To a cut of both Pomerons of the graph (Fig. 7a) there corresponds an inelastic process (Fig. 7c). In this case, the inclusive spectrum of the

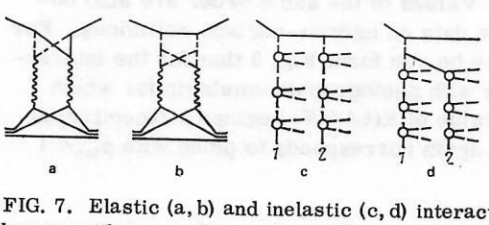

FIG. 7. Elastic (a, b) and inelastic (c, d) interaction of a fast baryon with two nucleons of a nucleus. The continuous line is the baryon, the broken line the meson.

mesons in ladder 1 is the same as in a hadron–nucleon collision, and the secondary baryon is softer, since some of its energy has been expended on the production of ladder 2. However, in the cut of the graph of Fig. 7b, which is shown in Fig. 7d, the secondary baryon is the same as in a collision with a nucleon but there are fewer fast mesons.

There are no grounds for restricting the consideration to only graphs of the type of Fig. 7a (i.e., Fig. 7c, an inelastic process), as is done in the leading-particle cascade model.[31-34] At the same time, the use of graphs of the type of Fig. 7c does not yet mean that only planar diagrams are taken into account. It is most natural to assume that the contributions of Figs. 7c and 7d should be of the same order. Then the multiplicity ratios of all fast particles (both baryons and mesons) on a nucleus and on a nucleon will be less than unity but greater than the ratio $\sigma_{abs}^{(1)}/\sigma_{abs}^{hA}$, i.e., all particles will be shadowed approximately equally. As can be seen in Fig. 4, just such behavior is observed experimentally. If the contribution of Fig. 7c is dominant, then, as was noted in Ref. 31, the multiplicity ratios of fast secondary particles on a nucleus and on hydrogen will be $\sigma_{abs}^{(1)}/\sigma_{abs}^{hA}$ for baryons and unity for mesons (i.e., the latter will not be shadowed at all). The data in Fig. 4 contradict this hypothesis. More detailed predictions about the behavior of the hard part of the spectrum will be made in the following section on the basis of the quark model.

In the target fragmentation region, there are two factors which significantly influence $R(hA/hN)$. First, $R(hA/hN)$ is increased by the Fermi motion of the nuclear nucleons. Second, a contribution from cascade rescattering of secondary particles is possible. As was noted in Refs. 61–63, both phenomena must be most clearly manifested in neutrino interactions or in deep inelastic electroproduction on nuclei, since in these cases the primary interaction takes place in the same way as on a free nucleon.[3)]

In Fig. 8a, which is taken from Ref. 64, we give the inclusive spectra of negatively charged particles in $\bar{\nu}$Ne and $\bar{\nu}p$ interactions. It can be seen that for $x_F > -0.25$ the spectra on the neon nucleus and on hydrogen do not differ. At smaller values of x_F, corresponding to π^- mesons with momenta $p_{lab} \lesssim 0.5$–0.8 GeV/c, the multiplicity on the nucleus becomes greater than on the proton. Figure 8b, which is taken from Ref. 65, shows the multiplicity ratios of particles whose sign is the same as the W boson's and of particles of opposite sign in ν and $\bar{\nu}$ interactions with Ne nuclei and with the nucleon. A departure from unity is observed only at $y \lesssim 1$–1.5, i.e., for pions with momenta less than 1 GeV/c. Values of the same order are also obtained from the data on hadron–nucleus collisions. For example, it can be see form Fig. 3 that for the interaction of protons with photographic emulsion for which $\langle\nu\rangle$ is 2.5 the value of $R(hA/hN)$ begins to exceed $\langle\nu\rangle$ at $\eta \lesssim 1.5$, which again corresponds to pions with $p_{lab} \leqslant 1$ GeV/c.

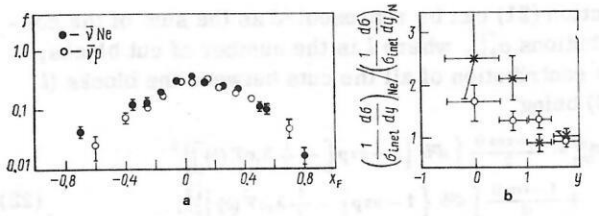

FIG. 8. Inclusive spectra of negatively charged particles in $\bar{\nu}$Ne and $\bar{\nu}p$ interactions (a) and ratios of the spectra of particles whose signs are equal to the sign of the W boson (open circles) and of particles of opposite signs (crosses) in ν, $\bar{\nu}$–Ne and ν, $\bar{\nu}$–N collisions (b).

Note that despite the common opinion cascade rescatterings are in no way related to the so-called enhanced graphs, which contain interaction of Reggeons with one another. For example, the enhanced graphs make a contribution (albeit a small one at the accessible energies) to the total interaction cross section, whereas the cascade rescatterings in no way affect the values of σ_{tot}^{hA} and σ_{prod}^{hA}.

Thus, from the point of view of the multiple-scattering model we can expect the existence at high energies of three rapidity regions with different behavior of $R(hA/hN)$:

1. The region of fragmentation of the nucleus, $y \lesssim 1$–2, $R(hA/hN) > \langle\nu\rangle_{hA}$ because of the Fermi motion and, possibly, cascade rescatterings.

2. The central region $(1\text{–}2) < y < Y - Y_0$, $R(hA/hN) = \langle\nu\rangle_{hA}$.[4)] Here, $Y - Y_0$ does not depend on the energy but increases with increasing A.[23]

3. The beam fragmentation region, $y \sim Y$, $\sigma_{abs}^{(1)}/\sigma_{abs}^{hA} < R(hA/hN) < 1$.

Because $R(hA/hN) < \langle\nu\rangle_{hA}$ in a considerable range of rapidities, the ratio of the mean multiplicities of the secondary particles is also less than $\langle\nu\rangle_{hA}$ and increases with increasing A slower than $A^{1/3}$.[23]

In Ref. 28, the inclusive spectra of secondary particles on nuclei were calculated in the multiple-scattering model. The results are given in Fig. 9 and are in good agreement with the experimental data.[67] The calculations of the inclusive spectra and the two-particle correlations made in Ref. 29 also agree with experiment.

However, the multiple-scattering model does not permit one to distinguish the species of the secondary particles. This, of course, is a shortcoming of it.

E. Multiplicity distributions of charged particles. If only particles with momenta $\lesssim 1$ GeV/c participate in cascade interactions, the number of relativistic particles n_s is hardly changed, and the multiple-scattering model makes it possible to calculate the n_s distributions in hadron–nucleus collisions at high energies.

[3)] This question is discussed in more detail in Sec. 7.

[4)] In reality, because of the departure from scaling in the central region of the spectrum in the case of scattering by nucleons,[66] the value of $R(hA/hN)$ must be somewhat less than $\langle\nu\rangle_{hA}$. The difference is discussed in Ref. 28.

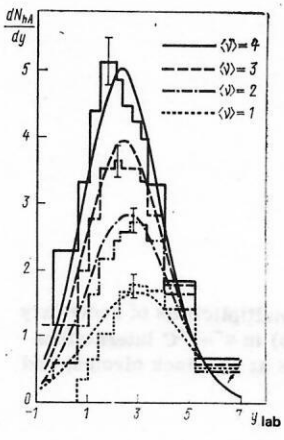

FIG. 9. Multiplicities of charged particles in hA interactions at 200 GeV as functions of y_{lab} for different values of the parameter $\langle\nu\rangle_{hA}$ (32).

For such a calculation, it is necessary to know how the energy E_0 of the initial particle is distributed in the cases when secondary particles are produced on several nucleons. As in Ref. 68, in which multi-Pomeron processes in hadron–hadron collisions were considered, we make the simplest assumption that in an inelastic interaction with ν nucleons each interaction occurs at the energy E_0/ν.[5)] Then the contribution of such a process to the multiplicity distribution will be determined by the $(\nu-1)$-fold convolution of the hadron–nucleon distributions, from which the contribution $hN \sim h^*N$ of diffraction production must first be subtracted. This convolution will occur with weight equal to $\sigma_{abs}^{(\nu)}/\sigma_{abs}^{hA}$. In the calculations, details of which are described in more detail in Ref. 23, allowance was made for the contributions of both the multiparticle (6) and the diffraction [(4) and (5)] processes. In contrast to Ref. 23, the expressions (18), (20), and (25) with the Fermi distribution (11) of the nuclear matter were used for nuclei with $A > 20$. For light nuclei, a Gaussian density distribution was used.[23]

The results of the calculations are compared in Fig. 10 with the experimental data on the interaction of protons at 400 GeV (Ref. 69) and 200 GeV (Ref. 70) and of 200-GeV π^- mesons[71] with photoemulsion nuclei. The agreement with experiment is fully satisfactory. At the values $n_s = 1.3$ and 5 (for π^-) a contribution of coherent production can be noted. A certain irregularity of the curves at $n_s \sim 10$ can be explained by taking into account hydrogen present in the emulsion. For comparison, the broken curves in Fig. 10 show the n_s distributions on a nucleon $N = \frac{1}{2}p + \frac{1}{2}n$ at the same values. Comparison of calculations in the multiple-scattering model with the data on p Em interactions at other energies[23] and with the n_- distributions in π^{-12}C collisions at 40 GeV/c (Refs. 72 and 73) and π^-Ne collisions at 25 and 50 GeV/c (Ref. 74) also led to good agreement with the experiments.

The experimental data on the ratios of the mean multiplicities of secondary particles on nuclei of carbon, photographic emulsion, and lead and on hydrogen are shown in Fig. 11 together with calculations in the multiple-scattering model. (The experimental data in Ref. 30 were used.) Overall, the agreement is reasonable, but the recently published data[75,76] for lead exceed the results of the calculation by 10–15%. The description may be improved by choosing a different way of taking into account energy conservation. For example, in Ref. 30, in which allowance was made for the quark with several nucleons the energy was divided in a geometric progression, good agreement with the $\langle n_s\rangle_{hA}$ data was achieved, including the data shown in Fig. 11. (This result is discussed in more detail in Sec. 5.) It must be recognized that the rules for distributing energy between the various interactions are not entirely clear and require further study.

The most characteristic feature in the multiple-scattering model is the increase in the ratio $\langle n_s\rangle_{hA}/\langle n_{ch}\rangle_{pp}$ with increasing energy, which is due to the de-

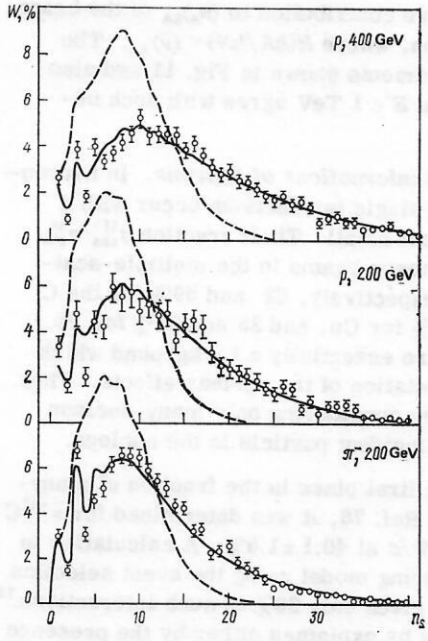

FIG. 10. Multiplicity distributions of relativistic charged particles in collisions of protons and π^- mesons with photoemulsion nuclei (continuous curves) and with the nucleon (broken curves).

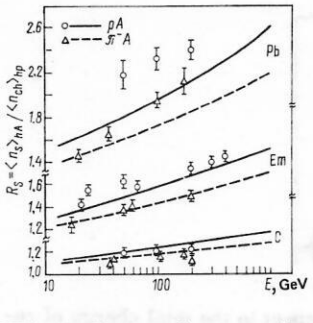

FIG. 11. Ratios of mean multiplicities of charged particles on nuclei and on hydrogen for proton and π^--meson beams as functions of the initial energy.

5) In Refs. 28 and 29, a different hypothesis was used.

crease in the relative contribution to $\langle n_s \rangle_{hA}$ of the beam fragmentation region, where $R(hA/hN) < \langle \nu \rangle_{hA}$. The results of the experiments shown in Fig. 11 and also cosmic-ray data[77] at $E \lesssim 1$ TeV agree with such behavior.

F. Many-nucleon interactions of hadrons. In hadron–nucleus collisions, single interactions occur with a probability that is not small. Their fraction $\sigma_{abs}^{(1)}/\sigma_{abs}^{hA}$ for proton and π^--meson beams in the multiple-scattering model is, respectively, 62 and 69% for the C nucleus, 38 and 47% for Cu, and 25 and 34% for Pb. Such interactions are essentially a background which reduces the manifestation of the nuclear effects. They can be eliminated by considering only many-nucleon interactions of the incident particle in the nucleus.

Of interest in the first place is the fraction of many-nucleon events. In Ref. 78, it was determined for $\pi^-{}^{12}$C collisions at 40 GeV/c at 40.1 ± 1.5%. A calculation in the multiple-scattering model using the event selection criteria in Ref. 78 gives only 33% of such interactions.[73] The difference may be explained either by the presence of fast nucleons ejected from the nucleus by virtue of the Fermi motion or by the contribution of cascade rescattering. Thus, the maximal contribution of the cascade processes, which transform single-nucleon interactions into many-nucleon interactions, does not exceed 7% for the ^{12}C nucleus.[73]

Many-nucleon π^-C interactions at 40 GeV/c were studied in more detail in Refs. 73 and 78 by means of a classification of events on the basis of the total electric charge Q of the relativistic secondary particles. In π^-p and π^-n collisions, Q can take the values −1, 0 and −2 and −1, depending on the presence of an identified proton (with $p < 700$ MeV/c). Events with other values of Q are classified as many-nucleon events. A similar analysis was also made in Ref. 74 for π^-Ne interactions at 25 and 50 GeV/c. Figure 12 shows the distributions, taken from Refs. 73 and 74, of the number of events with respect to Q together with the results of calculations, in which it was assumed that in 10% of the events there is one additional, positively charged relativistic particle. Only when allowance is made for such particles can the experimental data be described. Under the same assumptions, the mean multiplicities of all relativistic particles, $\langle n_\pm \rangle$, and of π^- mesons, $\langle n_- \rangle$, were calculated at different values of

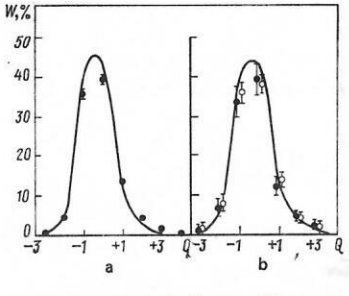

FIG. 12. Distributions with respect to the total charge of relativistic particles: a) in $\pi^-{}^{12}$C interactions at 40 GeV/c; b) in π^-–Ne collisions at 25 (black circles) and 50 (open circles) GeV/c.

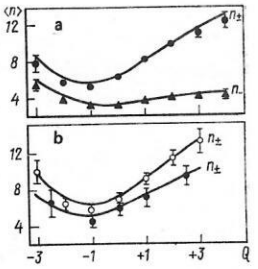

FIG. 13. Dependence of the mean multiplicities of secondary particles on their total charge Q: a) in $\pi^-{}^{12}$C interactions at 40 GeV/c; b) in π^-–Ne collisions at 25 (black circles) and 50 (open circles) GeV/c.

Q. They are given in Fig. 13. It can be seen that the calculations in the multiple-scattering model agree well with experiment even at large Q. However, this agreement is achieved only when allowance is made for the existence in every tenth event of an additional positively charged particle (evidently, a relativistic proton with $p > 700$–800 MeV/c) emitted either by virtue of the Fermi motion or by a cascade rescattering.

4. MANIFESTATION OF THE QUARK STRUCTURE OF HADRONS IN INELASTIC COLLISIONS WITH NUCLEI

A. Inelastic processes in the quark model. The composite quark model is based on the idea that mesons consist of two and baryons of three spatially separated objects, the constituent quarks. To maintain the correspondence with the parton model, it is assumed[79] that a constituent quark consists, in its turn, of a valence quark–parton surrounded by a cloud of quark–antiquark pairs and gluons. In contrast to point partons, such a constituent quark has a well-defined cross section for interaction with the target. In hadron collisions, the most frequent outcome is the interaction of one quark from each hadron, and the fraction of cases when several pairs of quarks interact will be assumed to be negligibly small.

In an inelastic collision, the constituent quark which has interacted "disintegrates." The point quark-partons in the sea group together or with the spectator quarks that did not interact and "grow" their own sea. Thus, secondary particles are produced, and these can be divided into two groups: the fragmentation particles, which contain the spectator quarks, and the particles in the central region of the spectrum, which consist solely of produced quarks. In the incident nucleon, each of the three constituent quarks has $x \sim 1/3$, and their x distribution is not very broad, so that there are two types of fragmentation baryon: B_{ij} with $x \sim 2/3$ containing two spectator quarks q_i and q_j, and B_i, which, like the fragmentation mesons M_i, contain one such quark q_i and have $x \sim 1/3$. Accordingly, ~1/3 of the initial momentum is distributed between all the particles of the central region. In the case of a meson beam, the fragmentation particles—the baryons B_i and the mesons M_i—carry $x \sim 1/2$ and the same fraction is distributed between all the particles of the central region.

The relations governing the production of the various fragmentation particles can be found by means of the combinatorial quark-counting rules proposed in Refs. 80 and 81. If quarks and antiquarks are captured from the sea with equal probability, the spectator quark q_i will go over into the baryon B_i with probability 1/3 and into the meson M_i with probability 2/3,[80,81]

$$q_i \to \frac{1}{3} B_i + \frac{2}{3} M_i. \tag{33}$$

In the case of two spectator quarks,[80,81]

$$q_i q_j \to \frac{1}{2} B_{ij} + \frac{1}{12} B_i + \frac{1}{12} B_j + \frac{5}{12} M_i + \frac{5}{12} M_j. \tag{34}$$

The comparison with experiment made in Ref. 82 showed that the relation (33) is reasonably satisfied in e^+e^- annihilation. At the same time, the multiplicity of baryons in the case of meson beams is experimentally much lower than is predicted by the expression (33). The problem can be avoided by introducing a suppression of baryon exchange in the t channel.[6)] We assume that after fragmentation of the meson the constituent spectator quark q_i captures an antiquark from the sea with probability β and a quark with probability $1-\beta$. Then it goes over into $\beta M_i + (1-\beta) q_i q$ and after further captures we obtain

$$q_i \to \frac{\beta}{1-\beta+\beta^2} M_i + \frac{(1-\beta)^2}{1-\beta+\beta^2} B_i. \tag{35}$$

In contrast, in the case of baryon fragmentation the two spectator quarks (q_i and q_j) capture quarks with probability β and antiquarks with probability $1-\beta$. Then

$$q_i q_j \to \beta B_{ij} + \frac{1}{2} \frac{(1-\beta)\beta^2}{1-\beta+\beta^2} B_i + \frac{1}{2} \frac{(1-\beta)\beta^2}{1-\beta+\beta^2} B_j + \frac{1-\beta}{2} \frac{2-2\beta+\beta^2}{1-\beta+\beta^2} M_i + \frac{1-\beta}{2} \frac{2-2\beta+\beta^2}{1-\beta+\beta^2} M_j. \tag{36}$$

The baryon and meson multiplicity ratios are most sensitive to the value of β at $x \sim 1/2$ in the case of meson beams. On the basis of (35) and the tables of Ref. 81, the ratio of the $\bar{\Lambda}$ and K_s^0 yields for a beam of π^- mesons is predicted to be $\sim 2(1-\beta)^2/\beta$ and the ratio of the Λ and K_s^0 yields for a K^--meson beam is $\sim 2.3(1-\beta)^2/\beta$. Their experimental values at 200 GeV/c for particles with $p_\perp \sim 0.07$ GeV/c are, respectively, 0.11 ± 0.01 and 0.135 ± 0.025,[83] which corresponds to $\beta \approx 0.8$.

B. Yields of fragmentation particles in pA collisions. The cross section for inelastic interaction of a constituent quark with a nucleon,

$$\sigma_q \equiv \sigma_{\text{inel}}^{qN} \approx \frac{1}{3} \sigma_{\text{inel}}^{NN} \approx \frac{1}{2} \sigma_{\text{inel}}^{\pi N} = 10 \text{ mb} \tag{37}$$

corresponds to a mean free path ~5 F in the nucleus, so that, as is shown in Fig. 14, when a hadron strikes a nucleus not only one but also two or three constituent quarks will "disintegrate." Then the number of fragmentation particles decreases and the multiplicity in the central region of the spectrum increases. The cross sections σ_n for the absorption of n constituent quarks in the case of a proton beam have the form[12]

$$\left.\begin{aligned} \sigma_1^p(A) &= 3\int d^2b \exp[-2\sigma q T(b)]\{1-\exp[-\sigma q T(b)]\}; \\ \sigma_2^p(A) &= 3\int d^2b \exp[-\sigma q T(b)]\{1-\exp[-\sigma q T(b)]\}^2; \\ \sigma_3^p(A) &= \int d^2b \{1-\exp[-\sigma q T(b)]\}^3, \end{aligned}\right\} \tag{38}$$

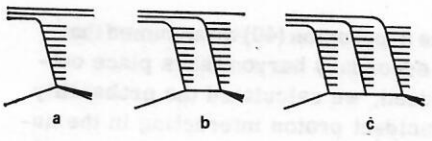

FIG. 14. Inelastic collisions of nucleons with nuclei. One (a), two (b), or all three (c) incident quarks interact.

where the function $T(b)$ is determined by the expression (9). The sum of the cross sections σ_1^p, σ_2^p, and σ_3^p with allowance for (37) is equal to $\sigma_{\text{prod}}^{pA}$ (10). Here, inelastic shadowing is not taken into account.

The probabilities of the processes of absorption of different numbers of quarks (Figs. 14a–14c) are

$$V_n^p(A) = \sigma_n^p(A)/\sigma_{\text{prod}}^{pA}. \tag{39}$$

These probabilities are directly related to the ratios of the yields of fragmentation particles on nuclei. Let us consider first the yields of baryons B_{ij} with $x \sim 2/3$. If one quark of the incident proton interacts with the nucleus (Fig. 14a), then the baryons B_{ij} are produced as in pp collisions. In the cases of Figs. 14b and 14c, the production of baryons with $x \sim 2/3$ is improbable, since we assume a small momentum spread of the quarks. Then the ratio of the multiplicities of the secondary baryons B_{ij} in pA and pp collisions must be[12]

$$R_{p\to B_{ij}}(x) = \frac{\sigma_{\text{inel}}^{pp} \frac{d^3\sigma}{d^3p}(pA \to B_{ij}X)}{\sigma_{\text{prod}}^{pA} \frac{d^3\sigma}{d^3p}(pp \to B_{ij}X)} = V_1^p(A), \tag{40}$$

and in the neighborhood of the point $x \sim 2/3$ this ratio should be independent of x.

Figure 15a shows the ratio $V_1^p(A)/V_1^p(\text{Cu})$ calculated in accordance with Eqs. (38) and (39), and also the experimental ratios of the multiplicities of protons[84,49] and Λ hyperons[50] with small transverse momenta on different nuclei and on the copper nucleus averaged in the interval $0.52 < x < 0.85$ for proton beam momentum 19.2, 24, and 300 GeV/c, respectively. The experiment agrees well with the results of the calculation.

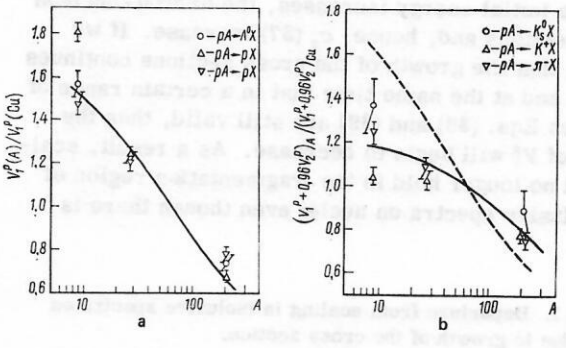

FIG. 15. Ratios of the multiplicities of secondary particles on different nuclei relative to the copper nucleus. a) Baryons in the interval $0.52 < x < 0.85$; the curve is calculated using Eqs. (38) and (39). b) Mesons at $x = 0.35$; the continuous curve is calculated using Eq. (42), and the broken curve is the result of calculation with instantaneous formation.

6) I am grateful of V. V. Anisovich and V. M. Shekhter for discussing this question.

Note that in using the expression (40) we assumed that the formation of the secondary baryon takes place outside the nucleus. Indeed, we calculated the probability of one quark of the incident proton interacting in the nucleus while the other two do not. However, the secondary baryon B_{ij} consists of three quarks and if it were formed within the nucleus one should take into account the possibility of absorption of the third quark. In this case, the ratio $R_{p\to\infty}(x\sim 2/3)$ for the nucleus Pb is 25% lower[12] than predicted by Eq. (40), and it does not agree with experiment.

In pA collisions, fragmentation mesons with $x\sim 1/3$ can be produced by the processes considered in both Figs. 14a and 14b. When allowance is made for the difference between the probabilities of capture of quarks and antiquarks for the case of Fig. 14b we find, as in the case of (35) and (36), that the spectator quark $q_i^{(B)}$ must go over into mesons and baryons in accordance with

$$q_i^{(B)}\to \frac{1-\beta}{1-\beta+\beta^2}M_i+\frac{\beta^2}{1-\beta+\beta^2}B_i. \tag{41}$$

Then ignoring the contribution from the decay of fast baryon resonances, we obtain the ratio of the multiplicities of mesons with $x\sim 1/3$ on the nucleus and on hydrogen in the form

$$R_{p\to M_i}(x\sim 1/3)=V_1^p(A)+\frac{1}{2-2\beta+\beta^2}V_1^p(A). \tag{42}$$

The dependence of $R_{p\to M_i}$ on β is rather weak. Thus, at $\beta=1/2$ we have $R_{p\to M_i}=V_1^p+0.8V_2^p$, and at $\beta=0.8$, $R_{p\to M_i}=V_1^p+0.96V_2^p$. The result of the calculation in accordance with Eq. (42) for the value $\beta=0.8$ is shown in Fig. 15b, in which we have also plotted the ratios of the multiplicities of π^- and K^+ mesons on different nuclei and on the Cu nucleus at $x=0.35$, taken from Ref. 84, and the K_s^0 multiplicities from Ref. 50. The agreement with experiment is perfectly satisfactory, but the calculation with instantaneous formation (broken curve) does not agree with experiment. Predictions for the ratios of the yields of fragmentation particles are also made in Ref. 12 for pion, kaon, and hyperon beams, but experimental data for sufficiently heavy nuclei are here virtually nonexistent.

As the initial energy increases, the hadron–nucleon cross sections and, hence, σ_q (37) increase. If we assume that the growth of the cross sections continues further and at the same time that in a certain range of σ_q values Eqs. (38) and (39) are still valid, then the values of V_1^p will begin to decrease. As a result, scaling will no longer hold in the fragmentation region of the inclusive spectra on nuclei even though there is scaling on hydrogen. The scale of the possible departures from scaling is illustrated in Table I. Such behavior can occur up to the onset of scaling violation in hadron–hadron and hadron–nucleus interactions because of the overlapping of the quarks within a hadron.[85]

TABLE I. Departure from scaling in inclusive spectra on nuclei due to growth of the cross section.

E_{lab}, GeV	$\sim 10^2$	$\sim 10^4$	$\sim 10^5$	$\sim 10^6$	$\sim 10^7$
σ_q, mb	10	13.5	15	17	20
V_1^p (^{14}N)	0.69	0.62	0.60	0.57	0.53
V_1^p (Cu)	0.47	0.39	0.37	0.34	0.31
V_1^p (Pb)	0.30	0.25	0.23	0.22	0.20

C. Multiplicity of the particles in the central region of the spectrum in pA and πA collisions. If the interaction between the quark–partons of the different constituent quarks can be ignored, the multiplicity in the central region in the case of the interaction of a proton with a nucleus, n_{pA}, is equal to the multiplicity in a quark–nucleus collision, n_{qA}, multiplied by the mean number of interacting quarks N_q^p:

$$R\left(\frac{pA}{qA}\right)=\frac{n_{pA}}{n_{qA}}=N_q^p=V_1^p+2V_2^p+3V_3^p$$
$$=\frac{3}{\sigma_{\text{prod}}^{pA}}\int d^2b\{1-\exp(-\sigma_qT(b))\}. \tag{43}$$

In the case of a pion beam, writing the probabilities of inelastic interaction of one or both quarks in a form analogous to (38) and (39), we obtain

$$R\left(\frac{\pi A}{qA}\right)=\frac{n_{\pi A}}{n_{qA}}=N_q^\pi=V_1^\pi+2V_2^\pi=\frac{2}{\sigma_{\text{prod}}^{\pi A}}\int d^2b\{1-\exp[-\sigma_qT(b)]\}. \tag{44}$$

Dividing (43) by (44), we obtain

$$\frac{\sigma_{\text{prod}}^{pA}}{\sigma_{\text{prod}}^{\pi A}}R\left(\frac{pA}{\pi A}\right)=\frac{3}{2}. \tag{45}$$

Figure 16 shows the experimental data on the ratios (45) for C and Pb nuclei[86] and $\frac{1}{2}$ Ag + $\frac{1}{2}$ Br (Ref. 10) at energy 200 GeV in their dependence on the quasirapidity η. In the range $1.5<\eta<3.5$, the relationship (45) is satisfied with good accuracy.

D. Inelasticity coefficients and the probabilities of inelastic charge exchange. To calculate the inelasticity coefficients, i.e., the fractions of the initial energy transferred to a given species of secondary particle, it is necessary to know the composition of the produced particles and their mean energy, which depends on the production mechanism. For example, the main contribution to the inelasticity coefficient K_γ (the fraction of the energy transferred to γ rays) is made by the γ rays from the decay of π^0 and η mesons, which can be produced both in the central region and in the projectile fragmentation region. In both cases, the π^0 mesons will be produced both directly from a quark–antiquark pair and by the decay of meson (ρ,ω,K^*) or baryon (Δ,Σ^*) resonances.

The relative multiplicities of the secondary particles of each species were calculated in accordance with

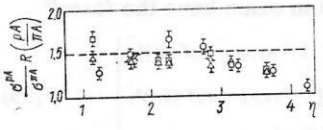

FIG. 16. The ratio (45) as a function of the quasirapidity η for different nuclei. The broken line shows the predictions of the quark model. The open triangles are for Pb, the open circles for $\frac{1}{2}$Ag + $\frac{1}{2}$Br, and the open squares for C.

Eqs. (35), (36), and (41) using the tables of Ref. 81, which determine the probabilities of the transition of quarks into the various hadrons; only the lowest multiplets of the group $SU(6)$ were taken into account: 36 for the mesons and 56 for the baryons. For a pion beam, it was assumed that the fragmentation hadron carries on the average half the initial energy, and in the case of baryon beam either one third (B_i and M_i) or two thirds (B_{ij}). The fraction of energy carried away by particles of a given species in the central region was assumed to be proportional to their multiplicity, and the fraction of energy transferred to the target fragmentation region was assumed to be negligibly small. At energies $\lesssim 10^3$ GeV, the production of baryon–antibaryon pairs in the central region was ignored.

The energy fractions carried away by all the positively charged, K_+ and negatively charged, K_-, secondary particles for proton and π^--meson beams were found to be

$$K_+^p(A)=0.46V_1^p(A)+0.35V_2^p(A)+0.30V_3^p(A);$$
$$K_-^p(A)=0.13V_1^p(A)+0.24V_2^p(A)+0.30V_3^p(A);$$
$$K_+^\pi(A)=0.23V_1^\pi(A)+0.30V_2^\pi(A);$$
$$K_-^\pi(A)=0.38V_1^\pi(A)+0.30V_2^\pi(A).$$

The numerical values of V_n^p and V_n^π for different nuclei are given in Ref. 12. For hydrogen in the framework of our approximation, $V_1^p=V_1^\pi=1$ and $V_2^p=V_3^p=V_2^\pi=0$, while for $A\sim150$–200 all the V_n are of the same order. Thus, it can be seen that the A dependences of all the inelasticity coefficients are very weak.

In Table II, we compare the theoretical calculations of the inelasticity coefficient K_γ with the data obtained in cosmic-ray experiments[87,88] for interactions of high-energy neutrons, π^+ mesons, and protons with nuclei. The agreement between the calculations and experiment is entirely satisfactory. The smaller value of K_γ in p Pb collisions at energies above 1 TeV (Ref. 88) could be due to the production of baryon–antibaryon pairs in the central region, which decreases the fraction of energy transferred to the γ rays. In the calculation of K_γ for this case, pair production was taken into account in the proportions $M:B:\bar{B}=6:1:1$.[80]

The quark model also makes it possible to calculate the probabilities of inelastic charge exchange, i.e., the fraction of events in which the electric charge of the fastest secondary particle (irrespective of its species) differs from the charge of the initial hadron. Of greatest interest is double charge exchange, when the charge difference is two. In meson–nucleon collisions, such processes must be almost completely determined by the production of fragmentation resonances ($\rho,\omega,K^*,\ldots$), as was noted earlier in Refs. 89 and 90. In the case of nuclear targets, an important contribution is also made by processes with absorption of both incident quarks, when all the secondary particles are produced from the sea.

TABLE II. Comparison of the calculated inelasticity coefficients K_γ (the lower numbers) with the experimental data (the upper numbers).

h	A			
	CH_2	Al	Fe	Pb
n, 200—2000 GeV	0.17±0.01 0.17	0.19±0.02 0.19	0.19±0.02 0.21	0.21±0.02 0.23
$\pi^\pm$, 200—2000 GeV	0.33±0,02 0.31	0.38±0.04 0.31	0,37±0.05 0.31	0.39±0.04 0.30
p, 10^3—$3\cdot10^4$ GeV	—	—	—	0.17±0.01 0.19

For a beam of π^- mesons, it follows from the quark-counting rules[81] with allowance for (35) that the ratio of the number of events in which the fastest particle is positively or negatively charged is

$$\frac{N_{\pi^-\to h^+}}{N_{\pi^-\to h^-}}=\frac{0.17V_1^\pi+0.30V_2^\pi}{0.43V_1^\pi+0.30V_2^\pi}.$$

If the contribution of the K mesons is ignored, this ratio can be expressed directly in terms of the multiplicities of the fragmentation π, ρ, and ω mesons. For nondiffraction π^-p collisions, we obtain

$$\frac{N_{\pi^-\to h^+}}{N_{\pi^-\to h^-}}=\frac{\langle n_{\rho^0}^f\rangle+0.6\langle n_\omega^f\rangle}{2\langle n_{\pi^-}^f\rangle+3\langle n_{\rho^0}^f\rangle+0.6\langle n_\omega^f\rangle}, \quad (46)$$

where $\langle n_f\rangle$ is the multiplicity of the direct mesons and it is assumed that $\langle n_{\rho^-}^f\rangle=2\langle n_{\rho^0}^f\rangle$. The expression (46) makes it possible to estimate the ratio of the yields of vector and pseudovector mesons in the fragmentation region.

5. THE MECHANISM OF QUARK–NUCLEUS INTERACTIONS AND THE STRUCTURE OF THE QUARK–QUARK AMPLITUDE

A. Multiple scattering of a quark within a nucleus. The results discussed in the previous section did not depend on the specific mechanism of the interaction of a constituent quark with a nucleus, which is of obvious interest. In accordance with (43) and (44), the ratios of the multiplicities of the secondary particles on nuclei and on the nucleon can be written in the form[10]

$$R\left(\frac{pA}{pN}\right)=\frac{n_{pA}}{n_{pN}}=R\left(\frac{pA}{qA}\right)\frac{n_{qA}}{n_{qq}};\ R\left(\frac{\pi A}{\pi N}\right)=\frac{n_{\pi A}}{n_{\pi N}}=R\left(\frac{\pi A}{qA}\right)\frac{n_{qA}}{n_{qq}},$$

where n_{qq} is the multiplicity in the central region in pN or πN collisions. The experimental ratios $R(pA/pN)$ and $R(\pi A/\pi N)$ are shown in Fig. 17, which is taken from Ref. 10. In the region $1.5<\eta<3.5$, where (45) holds, they are higher than $R(pA/qA)$ and $R(\pi A/qA)$, i.e.,

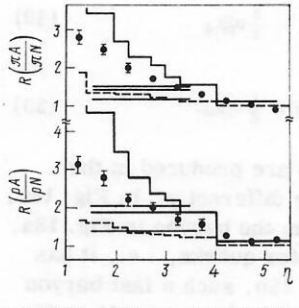

FIG. 17. Ratios of the multiplicities of charged particles on nuclei and on the nucleon as functions of η for p and π^- beams at 200 GeV. The black circles are for $\frac{1}{2}$Ag+$\frac{1}{2}$Br, the continuous steps are for Pb, and the broken steps for C. The straight lines show the values of $R(\frac{pA}{qA})$ (43) $R(\frac{\pi A}{qA})$ (45).

the multiplicity in the case of interaction of a quark with a nucleus is greater than in a quark–quark collision.

As was discussed in Ref. 91, there are two possibilities for explaining this phenomenon. One hypothesis attributes the difference between n_{qA} and n_{qq} to the contribution of the intranuclear cascades. Then the difference must be observed only for comparatively slow particles, which have time to form within the nucleus, while for the faster hadrons the ratio n_{qA}/n_{qq} is expected to be near unity. Another hypothesis attributes the difference between n_{qA} and n_{qq} to the interaction of a quark with several nucleons of the nucleus by the simultaneous emission of several ladders. In this case, n_{qA}/n_{qq} will be greater than unity everywhere except the quark fragmentation region, where it is important to take into account energy conservation. This variant is very similar to the multiple-scattering model discussed in Sec. 3. It corresponds to the presence in the amplitude of elastic quark–quark scattering of Regge cuts, whose contribution to the quark–nucleus amplitude increases strongly. At the same time, it is assumed that the interaction between the partons or the particles of the different ladders is weak.[92]

If the quark–nucleus interaction is described by the multiple-scattering model, then by analogy with (27) we can obtain the cross section for inelastic interaction of a constituent quark with different numbers ν of nuclear nucleons in the form

$$\sigma_{qA}^{(\nu)} = \frac{1}{\nu!}\int d^2b\,[\sigma_q T(b)]^\nu \exp[-\sigma_q T(b)]; \tag{47}$$

$$\sigma_{\text{prod}}^{qA} = \sum \sigma_{qA}^{(\nu)} = \int d^2b\,\{1-\exp[-\sigma_q T(b)]\}; \tag{48}$$

where $\sigma_{\text{prod}}^{qA}$ is the cross section for the production of secondary particles in a quark–nucleus collision. In a single interaction of a nucleon with a nucleus, any one of the three quarks interacts, and the other two remain spectators (Fig. 18a). With allowance for (37), the corresponding cross section

$$\sigma_{\text{prod}}^{(1)} = 3\int d^2b\,[\sigma q T(b)]\exp[-3\sigma_q T(b)]$$

is equal to $\sigma_{\text{prod}}^{(1)}$ (27). A double interaction can now occur in two ways. Two quarks can interact separately (Fig. 18b), or one quark may interact twice (see Fig. 18c). The contribution of these configurations are, respectively,

$$3\int d^2b\,[\sigma_a T(b)]^2\exp[-3\sigma_q T(b)] = \frac{2}{3}\sigma_{\text{prod}}^{(2)} \tag{49}$$

and

$$3\int d^2b\,\frac{1}{2}[\sigma_a T(b)]^2\exp[-3\sigma_q T(b)] = \frac{1}{3}\sigma_{\text{prod}}^{(2)}. \tag{50}$$

The fast secondary particles are produced in the processes in Figs. 18b and 18c differently. In Fig. 18c, baryon B in no way differs from the baryon in Fig. 18a, and it also contains two spectator quarks, i.e., it has $x \sim 2/3$; but in the case of Fig. 18b, such a fast baryon is improbable. On the other hand, the meson M in Fig. 18b is the same as in a single interaction, and in the process in Fig. 18c the meson will probably be softer. The processes in Figs. 18b and 18c strongly resemble the processes considered earlier in Figs. 7c and 7d,

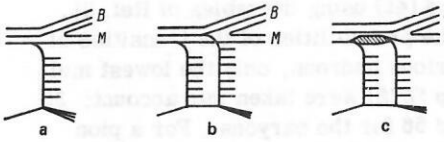

FIG. 18. Single (a) and double (b, c) interaction of a nucleon with a nucleus in the quark model.

and in the quark model the cross sections of the configurations in Figs. 18b and 18c bear the ratio 2 : 1 [Eqs. (49) and (50)].

Energy conservation is taken into account rather differently in the multiple-scattering model and in the quark model. Suppose the mean multiplicity of negatively charged particles in pN collisions at energy E_0 is

$$\langle n_-\rangle_{pN} = a + b\ln E_0.$$

In the multiple-scattering model,[23] it is assumed that the multiplicity in a double interaction is twice the multiplicity $\langle n_-\rangle_{pN}$ taken at half the energy, i.e.,

$$\langle n_-\rangle_{MP}^{(2)} = 2(a + b\ln E_0/2) = 2\langle n_-\rangle_{pN} - 2b\ln 2. \tag{51}$$

In the quark model in the case of a proton beam almost all the negatively charged particles are produced in the central region, so that $\langle n_-\rangle$ in the process in Fig. 18b is twice as large as in the case of Fig. 18a, and in the process in Fig. 18c we can, as in (51), take twice the multiplicity at the halved energy. Then we obtain

$$\langle n_-\rangle_{\text{QM}}^{(2)} = \frac{2}{3}2\langle n_-\rangle_{pN} + \frac{1}{3}[2\langle n_-\rangle_{pN} - 2b\ln 2] = 2\langle n_-\rangle_{pN} - \frac{2}{3}b\ln 2.$$

At $E_0 \sim 10^2$ GeV, $b \approx 0.9$, so that $\langle n_-\rangle_{\text{QM}}^2$ exceeds $\langle n_-\rangle_{\text{MSM}}^{(2)}$ by about 0.8.[7)] In collisions of higher order, the multiplicity in the quark model will also be higher than in the multiple-scattering model, which evidently improves the agreement with experiment in Fig. 11. However, this difference is not of a fundamental nature. One can choose a different way to take into account energy conservation; for example, one can assume that all proportions are equally probable[28,29] or that the energy is divided in a geometric progression.[30]

On the basis of the cross sections (47) and (48), it is easy to calculate the mean number of interactions of a constituent quark in the nucleus:

$$\langle\nu\rangle_{qA} = \frac{1}{\sigma_{\text{prod}}^{qA}}\sum_{\nu=1}\sigma_{qA}^{(\nu)} = \frac{A\sigma_q}{\sigma_{\text{prod}}^{qA}}. \tag{52}$$

The total number of interactions of a hadron within a nucleus is obtained by multiplying (52) by the mean number of interacting quarks: N_q^p (43) or N_q^π (44). In either case, we obtain a result which agrees with (32) after (37) has been taken into account. Note that this explains[30] the observed[75] dependence on $\langle\nu\rangle_{hA}$ alone of the ratio of the mean multiplicities of secondary particles on nuclei and on the nucleon.

Thus, the results of the multiple-scattering model and the quark model agree if a constituent quark can interact with either one or several nucleons (i.e., if

---

[7)] More accurate allowance for particle production in the beam fragmentation region[30] reduces the difference to 0.5.

there is an important contribution of cuts to the amplitude of elastic scattering of a quark by a nucleus).

B. Analysis of the mean multiplicities of secondary particles. In Ref. 30, an attempt was made to choose between the two hypotheses under discussion by analyzing the data on the multiplicities of secondary particles in hadron–nucleus collisions. If the multiplicities of the secondary particles in quark–nucleus and quark–nucleon interactions are equal (hypothesis A), the ratios of the multiplicities of the secondary particles in the central region and in the target fragmentation region must be equal to the mean number $N_q = \langle\nu\rangle_{hA}/\langle\nu\rangle_{qA}$ of interacting quarks. But if there is a multiple interaction of a quark in a nucleus (hypothesis B), then this ratio will be $\langle\nu\rangle_{hA}$.

To make a comparison with the experiments, the theoretically estimated multiplicities $\langle n^f_{\rm ch}(hN)\rangle$ of the particles in the beam fragmentation region were subtracted from the mean multiplicities in hA and hp collisions. In addition, allowance was made for the fact that in hadron–nucleus collisions some of the slow secondary particles are not included in the number $\langle n_s\rangle_{hA}$. The difference between interactions with protons and neutrons was also taken into account. It was then found that if the hypothesis A or B is correct, then then one must have, respectively,[30]

$$\xi_s^{(A)} = \frac{\langle\nu\rangle_{qA}}{\langle\nu\rangle_{hA}} \frac{\langle n_s(hA)\rangle - \langle n^f_{\rm ch}(hN)\rangle}{\langle n_{\rm ch}(hp)\rangle - 0.6 - \langle n^f_{\rm ch}(hN)\rangle} = 1; \quad (53)$$

$$\xi_s^{(B)} = \frac{1}{\langle\nu\rangle_{hA}} \frac{\langle n_s(hA)\rangle - \langle n^f_{\rm ch}(hN)\rangle}{\langle n_{\rm ch}(hp)\rangle - 0.6 - \langle n^f_{\rm ch}(hN)\rangle - D} = 1, \quad (54)$$

where the small value of $D = D(\langle\nu\rangle_{qA}, E)$ takes into account conservation of the energy if it is assumed to be divided in a geometric progression.

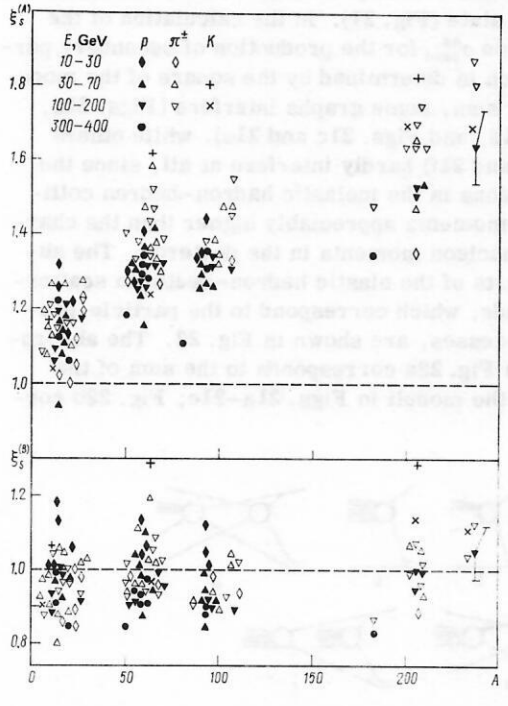

FIG. 19. Verification of the relations (53) and (54) for charged secondary particles.

The values of $\xi_s^{(A)}$ and $\xi_s^{(B)}$ for different beams and targets at energies above 10 GeV are given in Fig. 19, which is taken from Ref. 30. It can be seen that the relation (54) is satisfied with reasonable accuracy (the characteristic errors are shown on the right-hand side of the figure). The relation (53) is strongly violated, which may be explained by the contribution of particles produced in cascade interactions. The number of such additionally produced hadrons, $\langle n\rangle_{\rm add}$, can be found in each case by determining how many particles must be subtracted from $\langle n_s(hA)\rangle$ in the numerator of the expression (53) in order to obtain $\xi_s^{(A)} = 1$. For the case of proton and π^--meson collisions with nuclei in photographic emulsion, this number is given in Fig. 20, which is taken from Ref. 30, as a function of the initial energy. The growth of $\langle n(h\,{\rm Em})\rangle_{\rm add}$ with increasing energy, which is nearly logarithmic, does not accord well with the hypothesis of cascade interactions of secondary particles of moderate energy, since their number is almost independent of the initial energy. In addition, in the case of such a rapid growth of the contribution of the intranuclear cascades one would expect a simultaneous increase in the number of slower protons (which are included among the gray particles) than occurs experimentally.[93]

Thus, the data on the mean multiplicities of the charged particles favor hypothesis B, i.e., the assumption of multiple scattering of the quarks in the nucleus. A significant contribution of cascades to $\langle n_s\rangle_{hA}$ is not required, though there is a contradiction between the behavior of $\langle n_-(hA)\rangle$ for p and π^- beams.[30]

6. PROCESSES IN THE TARGET FRAGMENTATION REGION

A. Cascade rescattering of spectator quarks of the target. As we have shown, the observed phenomena in hadron–nucleus collisions can be explained by assuming that the interaction of the produced quark-partons within the nucleus is insignificant because of the long time required for their transition into new constituent quarks and secondary hadrons, so that virtually only the constituent quarks of the incident hadron interact. However, in the framework of such a scheme, the spectator quarks of the nuclear nucleons must also

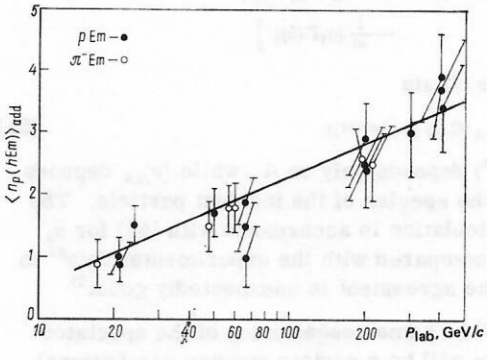

FIG. 20. Multiplicity of charged particles produced by intranuclear cascades on photoemulsion nuclei required to satisfy the relation (53) as a function of the initial energy.

interact within the nucleus. Once one of the quarks of a nuclear nucleon has interacted with a fast particle and "disintegrated" into partons, the other two quarks begin to move under the influence of the color forces and can undergo rescattering by other nucleons. The momenta of these constituent quarks must be of the same order (or probably somewhat less) than the momenta of the fragmentation particles B_{ij}, B_i, M_i in which they belong. The largest momentum in the laboratory system among these particles is possessed by the baryons B_i: $p \sim 1.5$ GeV/c at $p_\perp = 0.3$ GeV/c and ~2 GeV/c at $p_\perp = 0.7$ GeV/c (for $m_B = m_N$); however, in accordance with the quark combinatorial rules (36) the probability of their production is low (~1/5). The baryons B_{ij} and the mesons M_i, which are produced with a higher probability, have smaller momenta ($\lesssim$1–1.5 GeV/c), and therefore cascade interactions of the constituent quarks of the target should hardly change the multiplicity and other characteristics of the relativistic secondary particles. However, they may make an important contribution to the production of the gray particles (g). In such a case, their mean multiplicity, which depends on A as $\langle n_g \rangle \sim A^{2/3}$,[93] will be equal to the product of the mean number of constituent quarks knocked out of the target, which is equal to $2\langle \nu \rangle_{hA} \sim A^{1/3}$, and the mean number $\langle n_g \rangle^q$ of particles knocked out by one such quark.

In every inelastic hadron–nucleon interaction, there are two spectator quarks, and therefore $\langle n_g \rangle^q$ is the sum of half the mean multiplicity of the slow particles in an hN collision (these particles belong to the group of g particles), which is ~0.45 according to the estimate of Refs. 30 and 94, and the number of recoil protons ejected from the nucleus as a result of the scattering on them of a spectator quark. This last number can be taken equal to half the mean number of qN interactions, $\langle n_q^{\text{rescat}} \rangle$ (assuming that the number of protons is equal to the number of neutrons), and estimated in accordance with the expressions of the optical model. For example, the cross section of n-fold rescattering of particle 2 produced in the first interaction of particle 1 within the nucleus is

$$\sigma_{\text{rescat}}^{(n)} = \int \frac{d^2b\sigma_{1\to 2}}{\sigma_2 - \sigma_1} \exp[-\sigma_2 T(b)] \times \left\{ \left(\frac{\sigma_2}{\sigma_2 - \sigma_1}\right)^n [\exp[(\sigma_2 - \sigma_1) T(b)] - 1] - \left(\frac{\sigma_2}{\sigma_2 - \sigma_1}\right)^{n-1} [\sigma_2 T(b)] - \frac{1}{2!}\left(\frac{\sigma_2}{\sigma_2 - \sigma_1}\right)^{n-2} [\sigma_2 T(b)]^2 \dots - \frac{1}{n!} [\sigma_2 T(b)]^n \right\}.$$

Finally, we obtain

$$\langle n_g \rangle_{hA} = \langle \nu \rangle_{hA} [0.45 + \langle n_q^{\text{rescat}} \rangle]. \quad (55)$$

Here, $\langle n_q^{\text{rescat}} \rangle$ depends only on A, while $\langle \nu \rangle_{hA}$ depends on A and on the species of the incident particle. The results of calculation in accordance with (55) for $\sigma_2 = 10$ mb are compared with the experimental data[93] in Table III. The agreement is unexpectedly good.[8)]

Because of the same rescattering of the spectator quarks, there will be a certain number of additional protons with $p > 700$ MeV/c, and, as was required in Sec. 3, some of the single-nucleon events will be transferred to the group of many-nucleon events. But if the momenta of the spectator quarks do not, as a rule, exceed 1.5 GeV/c, then the protons ejected by them will have $p \lesssim 1$ GeV/c. Therefore, the number of faster protons must be proportional to $\langle \nu \rangle_{hA}$. This is confirmed by the experimental data.[95]

TABLE III. Comparison of calculated mean multiplicities $\langle n_g \rangle$ of gray particles with experiment at 200 GeV.

Data	$h-A$			
	p–CNO	p–Em	π^-–Em	p–AgBr
Theory [Eq. (55)]	1.1	2.4	2.0	3.2
Experiment (Ref. 93)	0.85±0.04	2.70±0.06	2.38±0.04	3.36±0.08

At energies ~1 GeV, the quark structure of the nuclear nucleons is not yet manifested. With increasing initial energy, it may happen that the main contribution to the target fragmentation process begins to be made by the mechanism of rescattering of the spectator quarks (and not the recoil nucleons), and then the longitudinal momentum transferred to the nucleus must be smaller. It could be that the transition to this new regime is responsible for the experimentally observed[96] abrupt change in the angular characteristics of the nuclear fragments when the initial energies are increased from 3 to 10–20 GeV and the subsequent constancy of these characteristics up to 300 GeV.

B. The fraction of double interactions in hadron–deuteron collisions. Rescattering of spectator quarks of the target is evidently also manifested in inelastic hadron–deuteron collisions at high energy.

Let us consider first processes without interaction in the final state (Fig. 21). In the calculation of the cross section $\sigma_{\text{prod}}^{hd}$ for the production of secondary particles, which is determined by the square of the modulus of their sum, some graphs interfere (Figs. 21a, 21b, and 21d, and Figs. 21c and 21e), while others (Figs. 21e and 21f) hardly interfere at all, since the recoil nucleons in the inelastic hadron–hadron collisions have momenta appreciably higher than the characteristic nucleon momenta in the deuteron. The absorptive parts of the elastic hadron–deuteron scattering amplitude, which correspond to the particle-production processes, are shown in Fig. 22. The absorptive part in Fig. 22a corresponds to the sum of the squares of the moduli in Figs. 21a–21c; Fig. 22b cor-

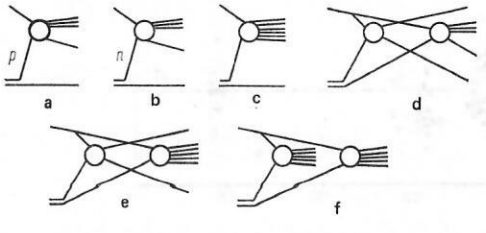

FIG. 21. Diffraction (a, b, d) and many-particle (c, e, f) processes in hadron–deuteron collisions.

[8)] Protons ejected from the nucleus as a result of the Fermi motion can also be included in the group of the g particles.

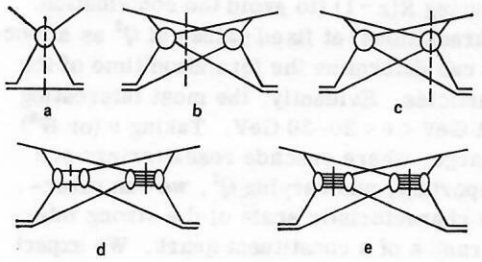

FIG. 22. Absorptive parts of the hadron–deuteron amplitude corresponding to inelastic processes (Fig. 21).

responds to the interference of the graphs in Figs. 21a and 21b; Fig. 22c shows the total contribution of the interferences of Figs. 21a and 21b with Fig. 21d, and also Fig. 21c with Fig. 21e; in Fig. 22d, we show the sum of the squares of the moduli of the graphs in Figs. 21d and 21e; finally, Fig. 22e corresponds to the square of the modulus of Fig. 21f. All these processes (apart from the one shown in Fig. 22b) are associated with cuts of one or two blocks of the hadron–nucleon interaction. A contribution to the cross section of the multiple processes from the cutting of one block is given by the graphs in Figs. 22a and 22c (the latter is the absorptive correction to Fig. 22a) and in accordance with (30) is

$$\sigma_{hd}^{(1,\,1)} = 2\sigma_{\text{in}} - 4\Delta_{\text{exp}}\sigma_{\text{in}}/\sigma, \tag{56}$$

where $\Delta_{\text{exp}} = \Delta_2$ is the experimental value of the shadowing correction to the total *hd* cross section. In the case of the cutting of two blocks, two cases are possible: elastic interaction with one nucleon and inelastic with the other (Fig. 22d):

$$\sigma_{hd}^{(2,\,1)} = 4\Delta_{\text{exp}}(\sigma_{\text{el}}/\sigma)(\sigma_{\text{in}}/\sigma), \tag{57}$$

and inelastic interaction with both (Fig. 22e):

$$\sigma_{hd}^{(2,\,2)} = 2\Delta_{\text{exp}}(\sigma_{\text{in}}/\sigma)^2. \tag{58}$$

Allowance for the finite range of the hadron–nucleon interaction changes (56)–(58) by not more than a few percent.

In the analysis of the experiments on multiple production in *hd* collisions made in Ref. 97, it was assumed that two types of process are possible—interaction with either one or both nucleons. In reality, as has been shown, there are three types of processes: (56), (57), and (58). In Regge language, the difference from Ref. 97 consists in allowance for the cuts in the *hN* amplitude, and although the processes (57) are to be classified in accordance with the experimental method of separating events as double interactions, σ_{double}, the mean multiplicity, like all the other characteristics, is here the same as in (56).

Allowance for the graphs in Fig. 23 with rescattering of the spectator quarks, i.e., with final-state interaction, does not change the value of $\sigma_{\text{prod}}^{hd}$. However, they make some of the events with single interaction into double processes. The fraction of such events depends on the cross section of the interaction of the spectator quark of the first nucleon with the second nucleon under the condition that the momentum transfer is not too

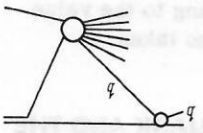

FIG. 23. Process with rescattering of a spectator quark of the target in the hadron–deuteron interaction.

small. We shall assume that this cross section is ~10 mb and that either of the two spectator quarks can be rescattered. To express the contribution of the graph in Fig. 23 in terms of the cross section $\sigma_{hd}^{(2,2)}$ (58), where the constant of the coupling to the second Reggeon is determined by a cross section ~30 mb in *pd* collisions and ~20 mb in πd collisions, it must also be borne in mind that the two graphs in Fig. 21f, in which the proton and neutron are interchanged, interfere, and the graphs in Fig. 23 are not present. Then the contributions to the cross section of double processes from the rescattering of spectator quarks are

$$\sigma_{pd}^{\text{rescat}} \approx \frac{1}{3}\sigma_{pd}^{(2,\,2)};\quad \sigma_{\pi d}^{\text{rescat}} \approx \frac{1}{2}\sigma_{\pi d}^{(2,\,2)}, \tag{59}$$

and the total cross section of double interactions is

$$\sigma_{\text{double}} = \sigma_{hd}^{(2,\,1)} + \sigma_{hd}^{(2,\,2)} + \sigma_{hd}^{\text{rescat}}. \tag{60}$$

The values of $\sigma_{hd}^{(2,\,1)}$, $\sigma_{hd}^{(2,2)}$, and $\sigma_{hd}^{\text{rescat}}$ are given in Table IV. For comparison, we also give the results of the calculations of Ref. 97 and the experimental data given there and also later in Ref. 98 on the cross sections of double interactions in *pd* and πd collisions. It can be seen that allowance for rescattering of the spectator quarks of the target explains the experimental data. If it is assumed that the particles produced in the central region have sufficient time to form and can also be rescattered, then the cross section of the double processes is clearly too large [since each pion makes a contribution of order $\sigma_{\pi d}^{\text{rescat}}$ (59)]. An attempt to explain the observed fraction of double interactions by rescatterings of secondary particles was made in the papers of Ref. 99, but in the first of them the calculations were made in the impulse approximation, and in the second the cross section $\sigma_{hd}^{(2,2)}$ was taken to be much smaller than in (58). As a result, to describe the experiments in Ref. 99 an appreciable

TABLE IV. Calculated cross sections of interactions with two nucleons in *hd* collisions and the experimental data. The values are given in mb.

hd	Δ_{exp}, Ref. 100	$\sigma_{\text{double}}^{\text{exp}}$, Refs. 97 and 98	Ref. 97	$\sigma_{hd}^{(2,1)}$, (57)	$\sigma_{hd}^{(2,2)}$, (58)	$\sigma_{hd}^{\text{rescat}}$, (59)	σ_{double}, (60)
pd 100 GeV	4.14±0.11	10.1±0.7	8.28±0.22	2.5	5.5	1,8	9,8
pd 200 GeV	4.26±0.11	9.9±1.0	8,52±0.22	2.5	5.7	1.9	10,1
pd 300 GeV	4.33±0.11	12.1±1.1	8.66±0,22	2.6	5.8	1.9	10.3
pd 400 GeV	4.45±0.15	12.4±0.8	8.90±0.30	2.7	5,9	2.0	10,6
$\pi^+ d$ 100 GeV	1.80±0.14	4.8±0.5	3.60±0.28	0.9	2.7	1.3	4.9
$\pi^- d$ 205 GeV	1.83±0.12	5.9±0.8	3,62±0.24	0.9	2.7	1.3	4.9
$\pi^- d$ 300 GeV	2.15±0.20	5.3±0.7	4.30±0.40	1.0	3,2	1.6	5.8

rescattering contribution, corresponding to the value $\mu^2 = 0.7$ GeV^2 in the expression (1), was taken.

7. THE SIZE OF A CONSTITUENT QUARK AND THE FORMATION TIME OF SECONDARY PARTICLES

A. The yields of secondary particles in deep inelastic processes on nuclei. As was pointed out in Sec. 3, the entire difference between deep inelastic interactions of leptons with nuclei and the free nucleon can be explained by the Fermi motion of the nucleons in the nucleus and rescattering of the secondary particles. Then the multiplicities of sufficiently fast secondary particles must be equal. However, the experiment of Ref. 101 on eA interactions in the range $7 \leqslant W^2 \leqslant 31$ GeV^2 at $\langle Q^2 \rangle \sim 1$ GeV^2 revealed an entirely different behavior. The multiplicities of fast particles (with $z = p_{\parallel}^{\text{cms}}/p_{\parallel\,\max}^{\text{cms}} \gtrsim 0.5$) produced on Sn and Cu nuclei were found to be 1.5–2 times less than for a deuterium target; at smaller z, the difference was somewhat less. There are two diametrically opposed explanations of this experiment. According to the one,[102] the entire difference is due to rescattering of secondary particles. For this, the parameter μ^2 in (1) must be taken equal to ~0.7 GeV^2, although such a large value of μ^2 must contradict the behavior of the multiplicities of the secondary baryons and mesons discussed in Sec. 4. In Ref. 103, the observed phenomena are attributed to absorption of a quark knocked out in the deep inelastic process.

There is a possibility of distinguishing between these two hypotheses by extending the range of variation of the variables Q^2 and ν and increasing the statistics. In the framework of the first hypothesis, an increase in the energy ν will increase the formation length of the fast secondary particles (with not too small z), and the formation length will finally become greater than the nuclear diameter. Then the ratio

$$R(z) = \left[\frac{dn}{dz}(\gamma^* + A \to h + X)\right] \Big/ \left[\frac{dn}{dz}(\gamma^* + d \to h + X)\right]$$

of the multiplicities of such particles reaches unity when $z > z_0$ and will not change any more. With increasing ν, the value of z_0 must decrease. In contrast, in the second model the ratio $R(z)$ is determined by the value of the quark–nucleon cross section and must therefore be virtually independent of ν. However, in the model of Ref. 102 it is assumed that the virtual γ ray interacts with point quark–partons, i.e., the value of Q^2 already appreciably exceeds the square of the reciprocal radius of a constituent quark, and therefore $R(z)$ must not depend on Q^2. In the model of Ref. 103, in contrast, it is actually assumed that it is not a point quark–parton which is knocked out of a nuclear nucleon but a constituent quark, which has a definite cross section for interaction with a nucleon and, therefore, a definite size. With increasing Q^2, the probability of such processes must decrease, since the interaction basically begins to take place with point quark–partons, and the value of $R(z)$ will tend to unity.

Thus, in both models we must expect the relation $R(z > z_0) = 1$ to hold at sufficiently large values of Q^2 and ν. Measuring $R(z \sim 1)$ (to avoid the contribution of multistep transitions) at fixed values of Q^2 as a function of ν, we can determine the formation time of the secondary particles. Evidently, the most interesting interval is ~1 GeV $< \nu <$ 20–50 GeV. Taking ν (or W^2) sufficiently large, where cascade rescatterings are already unimportant, and varying Q^2, we can determine the new characteristic scale of the strong interactions—the radius of a constituent quark. We expect the dependence

$$R(Q^2,\ z > z_0) = 1 - [1 - R_0(z > z_0)]\, F_q^2(Q^2), \qquad (61)$$

where $F_q(Q^2)$ is the form factor of the constituent quark and for Q^2 values which are not large can be represented in the form $F_q(Q^2) = 1 - 1/6 r_q^2 Q^2$, and

$$R_0(z > z_0) = \frac{\sigma_{\text{prod}}^{qA}}{A\sigma_q}$$

is the value of $R(Q^2)$ for $1/R_N^2 \ll 1/6Q^2 \ll 1/r_q^2$. According to the existing estimates, $r_q^2 \sim 0.5$–1 GeV,[104] and therefore the range ~1 $< Q^2 <$ ~30 GeV^2 is of greatest interest for verifying (61).

The rescattering of the ejected constituent quark must increase the multiplicity of the secondary particles compared with lepton–nucleon collisons, imitating an intranuclear cascade. Such an increase was observed in Ref. 105. When Q^2 is increased, the difference between $\langle n_s \rangle$ on nuclei and on the nucleon must decrease in proportion to $F_q^2(Q^2)$.

B. The formation time of the secondary particles. As can be seen from Fig. 15, the ratios of the yields of secondary baryons and mesons at high and medium energies are equal to within the errors. It follows from this that protons with $p \sim 10$ GeV/c and π^- and K^+ mesons with $p \sim 6$ GeV/c are formed outside the nucleus. This conclusion is confirmed by comparing the experimental data with the two calculated variants in Fig. 15b. Of course, the determination of the parameter μ^2 in (1) from the experimental data requires a special investigation, but its value can already be estimated roughly. The estimates of Ref. 106, made in the framework of the optical model, show that the effects of absorption in heavy nuclei begin to be manifested at formation lengths $l \sim 10$ F and become very important for $l < 7$–8 F; then we find from (1) that the value of μ^2 does not exceed 0.15–0.2 GeV^2. A bound of the same order is obtained by analyzing the energy dependence of the multiplicity of the fragmentation products of the nucleus, i.e., the gray and black prongs.[91]

An even stronger bound on μ^2 arises from the comparison of the yields of antiprotons and π^- mesons with momenta ~1 GeV/c in pA collisions.[106] This leads to values $\mu^2 \lesssim 0.03$–0.05 GeV^2. Nevertheless, as we pointed out in Sec. 6, a certain contribution of cascade rescatterings is neverthelss possible if one takes into account the already formed spectator quarks of the target. For a final decision concerning the formation time of the secondary particles, we evidently require fairly detailed data on deep inelastic electroproduction and neutrino processes on nuclei and a more detailed theoretical analysis.

CONCLUSIONS

At the present time, the picture of inelastic hadron–nucleus collisions at high energy is as follows. When a nucleus is struck, one, two, or three constituent quarks of the initial particle interact inelastically, the interactions taking place independently of one another. Each quark may interact with one or several nucleons, and in all the interactions it is essentially only those quarks present at the time of the collision in either the initial particle or the nucleons of the nucleus that participate. Such a picture agrees well with the available experimental data and suggests a number of predictions which can be tested experimentally.

In the framework of such ideas, important information was obtained about the properties of the strong interaction. Thus, it can be regarded as established that the secondary particles are not produced instantaneously but are formed during a certain time, this being fairly long from the point of view of the natural scales. There are very weighty arguments supporting the view that the matter within hadrons is distributed nonuniformly—the point quarks and gluons are grouped in two or three spatially separated clouds which have the quantum numbers of a valence quark. Finally, the quark–quark scattering amplitude is assumed to consist of a sum of several contributions, their relative magnitudes in the quark–nucleus interaction depending on A.

The most important tasks in the immediate future are to verify and make more accurate these results. It is necessary to establish the variables on which the formation time of the secondary particles depends, to establish whether the size of the constituent quarks is manifested in deep inelastic processes, to determine whether the strange constituent quark really does have a smaller cross section than the nonstrange quarks,[12] etc. For this, we need new experiments on the interactions of hadrons and leptons with nuclei at intermediate and high energies.

I thank V. V. Anisovich, V. G. Grishin, and V. M. Shekhter for valuable discussions.

[1]G. T. Zatsepin, Izv. Akad. Nauk SSSR, Ser. Fiz. **26**, 674 (1962).
[2]E. L. Feĭnberg, Zh. Eksp. Teor. Fiz. **50**, 202 (1966) [Sov. Phys. JETP **23**, 132 (1966)].
[3]C. Bemporad *et al.*, Nucl. Phys. **B33**, 397 (1971).
[4]R. P. Feynman, Photon–Hadron Interactions, Addison-Wesley, Reading, Mass. (1972) [Russian translation published by Mir, Moscow (1975)].
[5]V. N. Gribov, in: Materialy VIII Zimneĭ shkoly LIYaF (Proc. Eight Winter School of the Leningrad Institute of Nuclear Physics), Part 2, Leningrad (1973), p. 5.
[6]O. V. Kancheli, Pis'ma Zh. Eksp. Teor. Fiz. **18**, 465 (1973) [JETP Lett. **18**, 274 (1973)].
[7]A. S. Goldhaber, Phys. Rev. Lett. **33**, 47 (1974).
[8]V. V. Anisovich, Phys. Lett. **B57**, 87 (1975).
[9]A. Bialas, W. Czyz, and W. Furmanski, Acta Phys. Pol. **B8**, 585 (1977).
[10]V.V. Anisovich, F. G. Lepekhin, and Yu. M. Shabel'skiĭ, Yad. Fiz. **27**, 1639 (1978) [Sov. J. Nucl. Phys. **27**, 861 (1978)].
[11]N. N. Nikolaev, Phys. Lett. **B70**, 95 (1977).
[12]V. V. Anisovich, Ju. M. Shabelski, and V. M. Shekhter, Nucl. Phys. **B133**, 477 (1978); V. V. Anisovich, Yu. M. Shabel'skiĭ, and V. M. Shekhter, Yad. Fiz. **28**, 1063 (1978) [Sov. J. Nucl. Phys. **28**, 546 (1978)].
[13]A. Bialas and E. Bialas, Preprint FERMILAB-Pub-79/48-THY (1979).
[14]V. S. Barashenkov and V. D. Toneev, Vzaimodeĭstviya vysokoénergeticheskikh chastits i atomnykh yader s yadrami (Interactions of High Energy Particles and Nuclei with Nuclei), Atomizdat, Moscow (1972).
[15]V. S. Barashenkov and B. F. Kostenko, Preprint R2-11789 [in Russian], JINR, Dubna (1978).
[16]G.V. Davidenko and N. N. Nikolaev, Yad. Fiz. **24**, 772 (1976) [Sov. J. Nucl. Phys. **24**, 402 (1976)].
[17]E. M. Levin and L. L. Frankfurt, Pis'ma Zh. Eksp. Teor. Fiz. **2**, 105 (1965) [JETP Lett. **2**, 65 (1965)].
[18]H. J. Lipkin and F. Scheck, Phys. Rev. Lett. **16**, 71 (1966).
[19]N. N. Nikolaev and A. Yu. Ostapchuk, Preprint TH. 2575, CERN (1978).
[20]S. A. Voloshin, Yu. P. Nikitin, and P. I. Porfirov, Yad. Fiz. **31**, 762 (1980) [Sov. J. Nucl. Phys. **31**, 395 (1980].
[21]V. A. Abramovskiĭ and O. V. Kancheli, Pis'ma Zh. Eksp. Teor. Fiz. **15**, 559 (1972) [JETP Lett. **15**, 397 (1972)].
[22]K. A. Ter-Martirosyan, Itogi razvitiya redzhevskoĭ skhemy i éksperiment (Review of the Development of the Regge Scheme and Experiments), Engineering-Physics Institute, Moscow (1975).
[23]Yu. M. Shabel'skiĭ, Preprint No. 248 [in Russian], Leningrad Institute of Nuclear Physics (1976); Yad. Fiz. **26**, 1084 (1977) [Sov. J. Nucl. Phys. **26**, 573 (1977)]; Nucl. Phys. **B132**, 491 (1978).
[24]A. Capella and A. Kaidalov, Nucl. Phys. **B111**, 477 (1976).
[25]L. Bertocchi and D. Treleani, J. Phys. G **3**, 147 (1977).
[26]R. T. Cutler and D. R. Snider, Phys. Rev. D **13**, 1509 (1976).
[27]J. Weis, Preprint TH. 2197, CERN (1976).
[28]A. Capella and A. Krzywicki, Phys. Lett. **B67**, 84 (1977); Phys. Rev. D **18**, 3357 (1978).
[29]S. A. Azimov, Z. Phys. **A291**, 189 (1979).
[30]Yu. M. Shabelski and V. M. Shekhter, Acta Phys. Pol. **B11**, 317 (1980).
[31]N. N. Nikolaev and A. Ya. Ostapchuk, Preprint, L. D. Landau Institute of Theoretical Physics, Moscow (1978).
[32]S. A. Azimov *et al.*, in: Proc. of the First Workshop on Ultrarelativistic Nuclear Collisions (ed. L. Schroeder), LBL, Berkeley (1979).
[33]G. B. Alaverdyan *et al.*, Preprint R2-12536 [in Russian], JINR, Dubna (1979).
[34]K. Konoshita, A. Minaka, and H. Sumiyoshi, Preprint KYUSHU-79-HE-10 (1979).
[35]A. Z. Patashinskiĭ, Pis'ma Zh. Eksp. Teor. Fiz. **19**, 654 (1974) [JETP Lett. **19**, 338 (1974)].
[36]A. Afek *et al.*, in: Proc. of the Topical Meeting on Multiparticle Production on Nuclei at Very High Energies (ed. G. Bellini), ICTP, Trieste (1976), p. 591.
[37]F. Takagi, Preprint TU/78/188, Tohoku Univeristy (1978).
[38]É. V. Shuryak and O. V. Zhirov, Yad. Fiz. **28**, 485 (1978) [Sov. J. Nucl. Phys. **28**, 247 (1978)].
[39]K. Gottfried, Phys. Rev. Lett. **32**, 957 (1974).
[40]V. N. Kalinkin and V. L. Shmonin, Yad. Fiz. **21**, 628 (1975) [Sov. J. Nucl. Phys. **21**, 325 (1975)].
[41]N. Suzuki and S. Suzuki, Prog. Theor. Phys. **62**, 727 (1979).
[42]A. S. Carroll *et al.*, Phys. Lett. **B80**, 319 (1979).
[43]T. J. Roberts *et al.*, Nucl. Phys. **B159**, 56 (1979).
[44]D. S. Ayres *et al.*, Phys. Rev. D **15**, 3105 (1977).
[45]J. V. Allaby *et al.*, Yad. Fiz. **12**, 538 (1970) [Sov. J. Nucl. Phys. **12**, 295 (1971)].
[46]S. R. Denisov *et al.*, Nucl. Phys. **B61**, 62 (1973).
[47]S. A. Azimov *et al.*, Phys. Lett. **B73**, 500 (1978).
[48]E. S. Lehman and G. A. Winbow, Phys. Rev. D **10**, 2962 (1974).

[49]T. Eichten *et al.*, Nucl. Phys. **B44**, 333 (1972).
[50]P. Scubic *et al.*, Phys. Rev. D **18**, 3115 (1978).
[51]R. J. Glauber, High Energy Physics and Nuclear Structure, Amsterdam (1967).
[52]V. N. Gribov, Zh. Eksp. Teor. Fiz. **56**, 892 (1969); **57**, 1306 (1969) [Sov. Phys. JETP **29**, 483 (1969); **30**, 709 (1970)].
[53]V. N. Gribov and A. A. Migdal, Yad. Fiz. **8**, 1002 (1968) [Sov. J. Nucl. Phys. **8**, 583 (1969)].
[54]K. G. Boreskov, Protsessy rasseyaniya i obrazovaniya chastits pri vysokoĭ énergii v ramkakh teorii kompleksnykh momentov (Scattering and Production of Particles at High Energies in the Theory of Complex Angular Momenta), Author's Abstract of Dissertation for Candidate of Physical and Mathematical Sciences, Institute of Theoretical and Experimental Physics, Moscow (1970).
[55]P. M. Fishbane, J. G. Schaffner, and J. S. Trefil, Phys. Rev. D **10**, 3056 (1974).
[56]V. M. Kolybasov and L. A. Kondratyuk, Phys. Lett. **B39**, 439 (1972).
[57]V. Franco and R. J. Glauber, Phys. Rev. **142**, 1195 (1966).
[58]L. A. Kondratyuk, Yad. Fiz. **24**, 477 (1976) [Sov. J. Nucl. Phys. **24**, 247 (1976)].
[59]V. A. Abramovskiĭ, V. N. Gribov, and O. V. Kancheli, Yad. Fiz. **18**, 595 (1973) [Sov. J. Nucl. Phys. **18**, 308 (1973)].
[60]G. A. Winbow, Phys. Rev. D **15**, 3441 (1977).
[61]N. N. Nikolaev, Preprint, L. D. Landau Institute of Theoretical Physics, Moscow (1975).
[62]M. I. Strikman and L. L. Frankfurt, in: Fizika élementarnykh chastits. Materialy XIII Zimneĭ shkoly LIYaF (Elementary Particle Physics. Proc. 13th Winter School of the Leningrad Institute of Nuclear Physics), Leningrad (1978), p. 139.
[63]A. Bialas and W. Czyz, Nucl. Phys. **B137**, 359 (1978).
[64]J. P. Berge *et al.*, Phys. Rev. D **18**, 3905 (1978).
[65]T. H. Burnett *et al.*, Phys. Lett. **B77**, 443 (1978).
[66]W. Thome *et al.*, Nucl. Phys. **B129**, 365 (1977).
[67]C. Hallimwell *et al.*, Phys. Rev. Lett. **39**, 1499 (1977).
[68]K. A. Ter-Martirosyan, Phys. Lett. **B44**, 377 (1973).
[69]E. G. Boos *et al.*, Yad. Fiz. **28**, 697 (1978) [Sov. J. Nucl. Phys. **28**, 358 (1978)].
[70]Z. V. Anzon *et al.*, Yad. Fiz. **22**, 736 (1975) [Sov. J. Nucl. Phys. **22**, 380 (1975)].
[71]Z. V. Anzon *et al.*, Nucl. Phys. **B129**, 205 (1977).
[72]S. Batskovich *et al.*, Yad. Fiz. **26**, 554 (1977) [Sov. J. Nucl. Phys. **26**, 294 (1977)].
[73]N. S. Angelov *et al.*, Yad. Fiz. **28**, 999 (1978) [Sov. J. Nucl. Phys. **28**, 512 (1978)].
[74]Yu. M. Shabel'skiĭ and B. S. Yuldashev, Yad. Fiz. **31**, 1646 (1980) [Sov. J. Nucl. Phys. **31**, 854 (1981)].
[75]J. E. Elias *et al.*, Phys. Rev. Lett. **41**, 285 (1978).
[76]J. E. Elias *et al.*, Preprint FERMILAB-Pub-79/47 EXP (1979).
[77]O. L. Berdzenishvili *et al.*, in: Proc. of the 16th Intern. Cosmic Ray Conf., Vol. 6, Kyoto (1979), p. 204.
[78]N. S. Angelov *et al.*, Yad. Fiz. **26**, 811 (1977) [Sov. J. Nucl. Phys. **26**, 426 (1977)].
[79]V. V. Anisovich, in: Materialy IX Zimneĭ shkoly LIYaF (Proc. Ninth Winter School of the Leningrad Institute of Nuclear Physics), Part 3, Leningrad (1974), p. 106.
[80]V. V. Anisovich and V. M. Shekhter, Nucl. Phys. **B55**, 455 (1973).
[81]V. V. Anisovich, Yad. Fiz. **28**, 761 (1978) [Sov. J. Nucl. Phys. **28**, 390 (1978)].
[82]V. V. Anisovich, P. É. Volkovitskiĭ, and M. N. Kobrinskiĭ, Yad. Fiz. **29**, 1054 (1979) [Sov. J. Nucl. Phys. **29**, 543 (1979)].
[83]R. T. Edwards *et al.*, Phys. Rev. D **18**, 76 (1978).
[84]J. V. Allaby *et al.*, Preprint CERN 70-12, Geneva (1970).
[85]V. V. Anisovich and V. M. Shekhter, Yad. Fiz. **28**, 1079 (1978) [Sov. J. Nucl. Phys. **28**, 554 (1978)].
[86]W. Buza *et al.*, Paper submitted to the 28th Intern. Conf. on High Energy Physics, A2–45, Tbilisi (1976).
[87]S. A. Azimov *et al.*, Izv. Akad. Nauk SSSR, Ser. Fiz. **38**, 898 (1974).
[88]V. P. Pavlyuchenko *et al.*, Tr. Fiz. Inst. Akad. Nauk SSSR **109**, 30 (1979).
[89]K. G. Boreskov, A. B. Kaĭdalov, and L. A. Ponomarev, Preprint No. 950 [in Russian], Institute of Theoretical and Experimental Physics, Moscow (1972).
[90]B. Z. Kopeliovich and Ch. Tserén, Yad. Fiz. **26**, 643 (1977) [Sov. J. Nucl. Phys. **26**, 341 (1977)].
[91]Yu. M. Shabel'skiĭ, in: Fizika élementarnykh chastits. Materialy XIII Zimneĭ shkoly LIYaF (Elementary Particle Physics. Proc. 13th Winter School of the Leningrad Institute of Nuclear Physics), Leningrad (1978), p. 90.
[92]E. Lehman, Nucl. Phys. **B127**, 331 (1977).
[93]K. G. Gulamov, U. G. Gulyamov, and G. M. Chernov, Fiz. Elem. Chastits At. Yadra **9**, 554 (1978) [Sov. J. Part. Nucl. **9**, 226 (1978)].
[94]G. Calucci, P. Jengo, and A. Pignotti, Phys. Rev. D **10**, 1468 (1974).
[95]S. A. Azimov *et al.*, Materialy II Mezhdunar. seminara po problemam fiziki vysokikh énergiĭ (Proc. Second Intern. Seminar on Problems of High Energy Physics), D1, 2-12036, Dubna (1978).
[96]Ø. Scheidemann and N. T. Polile, Phys. Rev. C **14**, 1534 (1976); S. B. Kaufman, E. P. Steinberg, and M. W. Weisfield, Phys. Rev. C **18**, 1349 (1978).
[97]M. Baker *et al.*, Phys. Rev. Lett. **39**, 375 (1977); Phys. Rev. D **17**, 826 (1978).
[98]S. Dado *et al.*, Phys. Rev. D **20**, 1589 (1979).
[99]N. N. Nikolaev and V. R. Zoller, Phys. Lett. **B70**, 99 (1977); Nucl. Phys. **B147**, 336 (1979).
[100]A. S. Carroll *et al.*, Phys. Lett. **B61**, 303 (1976); **80**, 423 (1979).
[101]L. S. Osborne *et al.*, Phys. Rev. Lett. **40**, 1624 (1978).
[102]N. N Nikolaev, Preprint TH 2792 CERN, Geneva (1979).
[103]G. Nilsson, B. Anderson, and G. Gustafson, Phys. Lett. **B83**, 379 (1979).
[104]V. V. Anisovich, in: Fizika vysokikh énergiĭ. Materialy XIV Zimneĭ shkoly LIYaF (High Energy Physics. Proc. 14th Winter School of the Leningrad Institute of Nuclear Physics) (1979), p. 3.
[105]L. Hand *et al.*, Acta Phys. Pol. **B9**, 1087 (1978).
[106]A. O. Vaĭsenberg *et al.*, Pis'ma Zh. Eksp. Teor. Fiz. **29**, 719 (1979) [JETP Lett. **29**, 658 (1979)].

Translated by Julian B. Barbour